Journal of Hazardous Materials 465 (2024) 133214

Contents lists available at ScienceDirect

Journal of Hazardous Materials

journal homepage: www.elsevier.com/locate/jhazmat

Research Paper

Origin, spatial distribution, sediment contamination, ecological and health risk evaluation of trace metals in sediments of ship breaking area of Bangladesh

Asma Binta Hasan [a], A.H.M. Selim Reza [a,*], Md. Abu Bakar Siddique [b], Md. Ahedul Akbor [b], Aynun Nahar [b], Mehedi Hasan [b], Md. Ripaj Uddin [c], Mohammad Nazim Zaman [c], Iftekharul Islam [a]

[a] Department of Geology and Mining, University of Rajshahi, Rajshahi 6205, Bangladesh
[b] Institute of National Analytical Research and Service (INARS), Bangladesh Council of Scientific and Industrial Research (BCSIR), Dhanmondi, Dkaka 1205, Bangladesh
[c] Institute of Mining, Mineralogy and Metallurgy (IMMM), Bangladesh Council of Scientific and Industrial Research (BCSIR), Joypurhat, Bangladesh

HIGHLIGHTS

- Sediments were highly contaminated by Pb, Cd, Zn, Cu, As and Ag.
- Most of the sampling sites are highly polluted.
- The Cd has the highest while Pb and As had moderate ecological risk.
- Children had higher carcinogenic risk.
- Most of the trace metals exhibited anthropogenic origins.

GRAPHICAL ABSTRACT

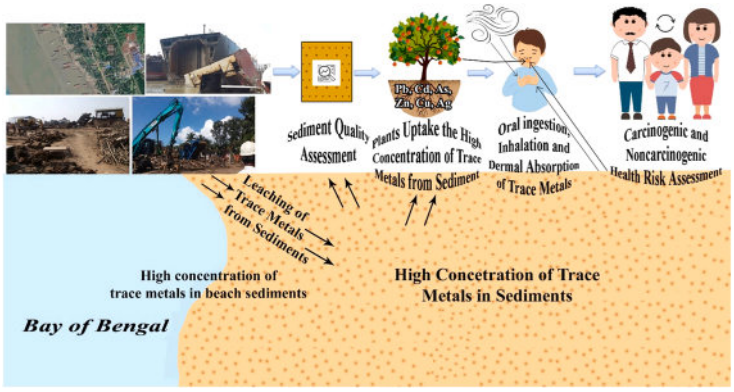

ARTICLE INFO

Editor: Edward Burton

Keywords:
Bangladesh
Ship breaking
Sediment pollution indices
Carcinogenic risk
Monte Carlo simulation

ABSTRACT

Eleven trace metals (Cd, Cr, Fe, Mn, Cu, Ni, Co, Zn, As, Pb, and Ag) in sediments of Bangladesh's ship breaking area were measured by an atomic absorption spectrometer to determine origin, contamination extent, spatial distributions, and associated ecological and human health hazards. This study found considerable quantities of Pb, Cd, Mn, Zn, and Cu when compared with standards and high levels of Pb, Cd, Zn, Cu, As, and Ag contamination according to pollution evaluation indices. Different indices indicate most of the sampling sites were highly polluted. However, spatial distribution maps indicate that trace metals were predominantly deposited in the northern and southern region. The ecological risk index revealed that Cd has the highest while Pb and As had moderate risk. Based on the health index values, Zn for both adults and children were higher than the safe limit while Mn, Pb, Cr, As, Fe, Cu, Ni, and Co for children were close to the threshold. The mean total carcinogenic risk

* Corresponding author.
E-mail address: sreza69@yahoo.com (A.H.M.S. Reza).

https://doi.org/10.1016/j.jhazmat.2023.133214
Received 2 October 2023; Received in revised form 17 November 2023; Accepted 7 December 2023
Available online 12 December 2023

values of Cr, As, and Ni for children and Ni for adults exceeded the permissible threshold. The cancer risk possibilities were further assessed using Monte Carlo simulation. Most trace metals have anthropogenic origins, which were attributed to ship breaking activities.

1. Introduction

Due to their enormous economic profit, the ship breaking and recycling industries are a growing sector of the global economy [1,2]. The process of "ship scrapping" entails removing the structural components of an old ship and turning them into salvageable elements like iron, aluminum and steel [2–7]. Dismantling is vital for sustainable growth not just to maintain a modern maritime fleet but also to keep a continuous flow of ecologically beneficial goods [9]. However, ship breaking is a difficult process due to the complexity of ship structures as well as the numerous environmental, safety and health concerns involved [11,12]. As a labor-intensive industry, ship breaking and recycling was too expensive in wealthy nations. Thus, during the early 1980 s, ship owners scraped their ships in the scrapyards of India, Pakistan, China, Vietnam, the Philippines, and Bangladesh to reduce the cost and maximize the profit [8,14]. Since that time, ship recycling or breaking has boosted Bangladesh's economy by fostering the steel, shipbuilding, furniture, building construction, mechanical, and electrical sectors [13]. Bangladesh has increasingly been involved in ship breaking over the past ten years, indicating the nation's progress towards becoming a world leader in this industry [9]. Its success is the consequence of a number of reasons, including government assistance, affordable labor, ideal beach conditions, high consumer demand for recovered items and most importantly inadequate environmental oversight [2,8,9,15,16]. Fig. 1 shows intensive ship breaking activities of Bangladesh.

Anyway, ship dismantling is a cause for worry in Bangladesh owing to its economic importance and environmental risks [17]. Until now, our nation had primarily focused on the financial benefits of ship-breaking yards, despite the fact that the extraction procedures involved pose a persistent threat to the environment and public health [2,18]. Cadmium (Cd), Lead (Pb), chromium (Cr), arsenic (As), mercury (Hg), manganese (Mn), zinc (Zn), nickel (Ni), copper (Cu) etc., are trace metals that are present in various parts of end-of-life ships [2,6,8,10,16,19,20]. During cutting of retired ships, diverse types of wastes including trace metals initially gathered over the beach sediment then eventually moving to the tidal, sub-tidal, deep seawaters and related sediments [3,4,21,22] and these are significant worries about in coastal ecosystems [19,23]. Because similar to a clogged sink, they can gradually release the collected trace metals into the surrounding water through various processes which can result in serious pollution and long-term harm to the aquatic ecosystem [24–27].

Trace metal poisoning of sediment is now a major environmental hazard on a global scale as a result of the world's growing industrialization [28]. Due to their toxicity, prolonged atmospheric persistence, and ability to bio-accumulate in the human body, trace metals are widely known environmental pollutants [2,26] and their exposure is primarily caused by trace metal-contaminated sediment [28]. Therefore, trace metal contamination of terrestrial and aquatic ecosystems is a serious environmental problem that negatively affects human health [29–32] and the least developed countries, such as Bangladesh, have a very difficult time addressing trace metal pollution [2,29,33–36]. The hydro-litho-biosphere interface is where sediment pollution offers a severe risk to ecosystems because sediments serve as both a source and a sink for pollutants in aquatic systems [8,37,38]. As a result of sediment losing its biological and chemical quality due to toxic metal pollution, ecosystems and humans are placed in risk [39,40]. This is due to the fact that contaminants in contaminated soil may be transferred to plants and affect crop development and food safety [28,41,42]. Moreover, trace metals may affect the soil's biology, functionality, and nutritional content [43–45]. Chemical elements have been categorized into a wide range of groupings, including those that are essential (Cu, Zn, Fe, Mn, Co, etc.) and potentially harmful (Pb, Cd, Cr, As, Hg etc) [46]. If the necessary element's concentrations go above certain thresholds, they can also cause toxicity [45]. Additionally, due to the ease with which elemental ions can enter an animal or human body through dermal absorption, inhalation, or ingestion, sediment with high concentrations of harmful elements poses a risk to both their health and that of humans

Fig. 1. Some photographs of ship breaking activities in Bangladesh.

and other animals [45,47]. Trace metals, even in small quantities, are extremely detrimental to the human body due to a lack of an efficient elimination mechanism [48]. Long-term exposure to Cd, for instance, may result in lung cancer, renal issues, hypertension, and prostatic proliferative lesions sand bone fractures. Arsenic inhalation may cause skin lesions, and long-term oral As exposure can lead to lung cancer [23]. The central nervous system may be hampered by the leaching of Pb, which can also cause anemia, plumbism, nephropathy, and gastrointestinal colic [49]. On the other hand, reputable research organizations like the USEPA (United States Environmental Protection Agency) and the IARC (International Agency for Research on Cancer) have previously designated hexavalent chromium as a human carcinogen [23].

Recent years have seen the completion of several independent research on the distribution of toxic metals and the degree of their pollution in surface sediments of the ship-breaking region [3,12,16,19,23,28,50]. Yet, every study differs based on the precise objectives of the investigation. As an example, Hasan et al. (2020) [28] assessed the amount of heavy metal concentrations in soil and frequently cultivated food crops, their transfer coefficient from soil to food crops, and any possible danger to human health connected with consuming these food crops. Heavy metal pollution was assessed by Rahman et al. (2019) [23]. Hossain et al. (2021) [19] investigated the pollution brought on by heavy metals as well as the qualitative and quantitative vertical distribution of heavy metals in core sediments. Alam et al. (2019) [16] calculated the concentrations of potentially toxic elements, their seasonal variations, and potential health risks from potentially toxic elements in the soil of the ship breaking area; Aktaruzzaman et al. (2014) [12], calculated the concentrations of heavy metals in water and sediment sample of the ship breaking site and their potential ecological risk; Hasan et al. (2013a) [3], looked at the spatial distributions of trace metals in sediments of the ship breaking area.

The majority of earlier publications used a small number of statistical data analysis techniques and a restricted numbers of factors to illustrate the scenario of toxic metal pollution of sediments. Nevertheless, no exhaustive research describing the degree of trace metal pollution in sediments, their spatial distributions, and their impacts on the environment and human health has been published yet. Therefore, we aim to (a) assess the levels of sediment contamination using several indices and their spatial distributions (b) evaluate potential ecological risks (c) estimate non-carcinogenic human health risk and carcinogenic health risk with Monte Carlo simulation, and (d) pinpoint the probabilistic sources of these metals.

2. Materials and methods

2.1. Study area and general geology

Sitakunda is an administrative part located in the northern part of Bangladesh's Chittagong district with a total area of 4894 km^2. It lies in the middle of the coordinates of 22°37′ N and 91°39.7′ E. [10]. Sitakunda boasts the world's second-largest ship breaking business even though it is mostly an agricultural region [28]. Attributable to its topographical, geological as well as its economic benefits, including a long, consistent intertidal shoreline with tidal variations of 6 m, the Sitakunda coastline and the nearby region are mostly used for ship-breaking operations [1,2]. The entire ship-breaking zone, covering an area of more than 20 km2 and located between 22°22′19.2′ and 22°33′43.2′ N, and 91°39′18′ and 91° 45′7.2′ E, was the subject of this investigation (Fig. 2).

The Sitakunda geological structure is one of the westernmost formations of Chittagong and the Chittagong Hill Tracts, measuring 70 km (43 miles) long and 10 km (6.2 miles) broad [51]. The studied region is tectonically a part of the Bengal Basin's folded flank's western mild sub-zone. This sub-zone is occupied by the Sitakund anticline, a box-shaped, doubly plunging, elongated, and asymmetrical anticline that is bordered by the Feni, Karnaphuli, Halda, and Sandwip rivers to the north, south, east, and west, respectively. It is situated on the Bangladesh's most seismically active faults known as Sitakunda-Teknaf fault. Therefore, cyclones, storm surges and earthquakes are natural hazards to this region [6]. Based on structure, topography, and rock type, Sitakund and the surrounding region are split into four separate physiographic units: the western coastal belt, the western alluvial plain, the central tertiary hills, and the eastern halda valley. The research region is located west of the western alluvial plain and is a part of the western coastal belt. This area is stretched out and thin, with a NNW-SSE trend. The average elevation in this low relief region is 0.41 m AMSL. This band may be represented as a region of submerged hills. A deep sedimentary succession of sandstone, shale, and siltstone is included in the structure. The exposed sedimentary rock strata, apart from limestone, are an average of 6500 m (21,325 ft) thick and do not vary in terms of the general lithology between Chittagong and Chittagong Hill Tracts region [52]. This area has hot, humid summers from April to June, followed by a warm, humid monsoon from July to September. South-southeasterly winds are more common from April to September and from October to March, northerly and north-easterly winds with mild winters are more common [10]. The region's yearly average temperature ranges from 32.5° to 13.5°C, and its mean monthly rainfall is 257.77 mm, with July seeing the greatest total of 726.9 mm [16].

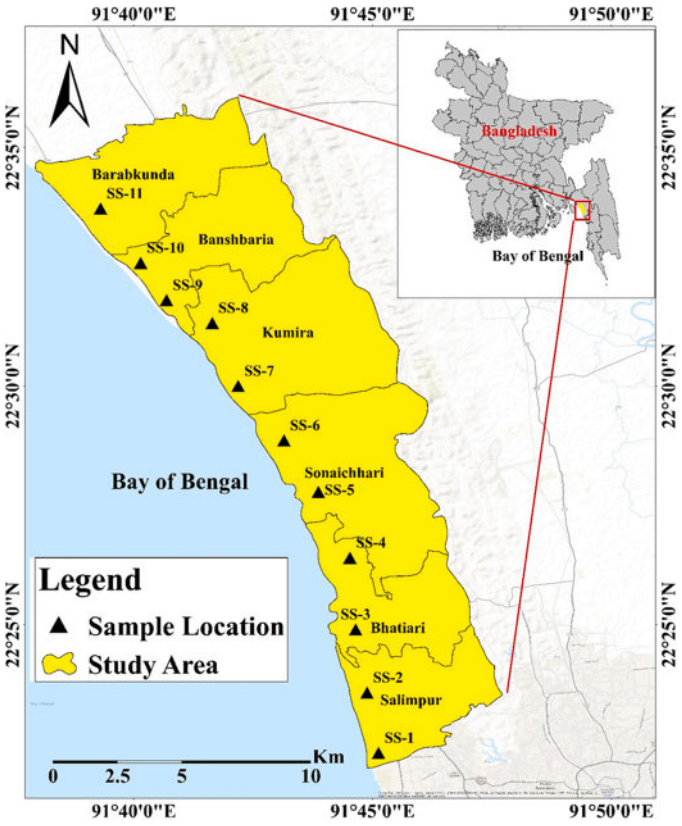

Fig. 2. Location map of the study area.

2.2. Sample collection and preparation

Sediment samples were taken from 11 sampling locations in and around the ship breaking zone throughout six consecutive unions of Bangladesh's Sitakunda upazilla in the Chattogram district. Using a large, clean stainless-steel spade, samples were randomly collected in triplicates (n = 3) from two sampling locations of each union (aside from one from Barabkunda) at several points horizontally from Salimpur to Barabkunda at intervals of approximately 1–3 km from the first sample site (Fig. 2). After collection, all samples were immediately

packed airtight in clean zip-lock plastic bags with the appropriate labeling to prevent any weathering and contamination.

After carefully bringing them into the lab, they were spontaneously dried by natural air for 7 days at room temperature, and then dried in an oven for 24 h at 110 °C [28,53]. Rocks, wooden pieces, and other non-sediment material were removed, and other obvious contaminants in the sediment were further filtered out. After being thoroughly homogenized and crushed in a clean mortar with a pestle, the samples were run through a 2 mm nylon mesh sieve. Then, the samples were preserved in zip-lock polythene bags that were airtight and kept at 4 °C until analysis [53].

After that, 10 g of uniformed sediment samples were digested in earlier washed and dried 250 mL beakers using a concentrated nitric acid (20 mL) and per chloric acid (10 mL) combination [28,54]. Beakers containing the ingredients for digestion were placed on a hot plate and heated at between 150 and 180 °C while being covered with a watch glass. After some time, the residual trace organic material was evaporated to produce a clean solution. After completely washing the first sample beaker with deionized water, the samples were transferred to a second 250 mL washed and dried beaker, where they were filtered using WhatmanTM qualitative 1 filter paper (125 mm dia.*100 circles). After adding 2 mL of concentrated HNO_3 to bring the volume of the filtrate sample solutions up to 50 mL, they were re-heated on the hot plate at 150°C-180°C. Transparent sample solutions were shifted to 100 mL calibrated volumetric flasks, cooled to room temperature, and filled to the designated level using sterile deionized water. Before filtering the sample solution into clean, labeled 200 mL translucent plastic bottles, we gave it a good stir and agitation to ensure that it was distributed evenly. A blank sample (in the absent of sediment samples) was also made ready in similar way for quality assurance. The samples were then stored in the lab at 4 °C until elemental analysis is performed [28].

As indicated in our earlier study, we took great care to ensure that the quality of the analysis was maintained sample gathering to laboratory evaluation [28]. Deionized water (electrical conductivity 0.2 μScm^{-1}, resistance 18.2 MΩ cm at 25 °C) and analytical-grade chemicals such HNO_3, $HClO_4$, H_2O_2 and HCl were used for sample preparation (Scharlau, Spain). The volumetric flask, pipette, and other glassware used in the experiment were all calibrated, and before to use, they were cleaned by soaking in 10% (v/v) HNO_3 for an entire night, followed by a rinse in deionized water. The GR-200 from A&D Company Ltd in Tokyo, Japan served as the digital electrical balance used to weigh the samples.

2.3. Sample analysis

The Institute of National Analytical Research and Service (INARS), Bangladesh Council of Scientific and Industrial Research (BCSIR), in Dhaka, Bangladesh, conducted analyses of sediment sample ~~analyses~~ for the elements Cd, Pb, Cr, Ni, As, Fe, Mn, Zn, Cu, Co, and Ag. This lab is accredited in accordance with ISO/IEC 17025:2017 [28,45,55]. All potential sources of sample contamination were mitigated by taking precautions throughout collection, transit, and storage, as well as during

Table 1
Trace metal concentrations in sediment samples of the ship breaking area, Bangladesh with their measurement uncertainty (±) and comparison of these with standard, background and some reference values.

Sample ID	Pb (mg/kg)	Cd (mg/kg)	Cr (mg/kg)	Fe (mg/kg)	Mn (mg/kg)	Zn (mg/kg)	Cu (mg/kg)	Ni (mg/kg)	Co (mg/kg)	As (mg/kg)	Ag (mg/kg)
SS-1	100.6 ± 0.4	1.61 ± 0.02	64.4 ± 0.4	10107.2 ± 2.4	930.7 ± 2.4	1146.3 ± 0.6	261.6 ± 0.4	85.7 ± 0.4	10.07 ± 0.06	4.01 ± 0.23	0.21 ± 0.04
SS-2	137.6 ± 0.6	1.67 ± 0.14	15.1 ± 0.2	10416.5 ± 1.4	1076.4 ± 3.2	1309.8 ± 0.2	367.9 ± 0.3	27.4 ± 0.4	13.91 ± 0.12	4.02 ± 0.04	0.29 ± 0.04
SS-3	68.3 ± 0.31	1.76 ± 0.22	63.1 ± 0.31	9489.7 ± 1.4	639.1 ± 1.6	949.8 ± 0.5	61.9 ± 0.3	20.9 ± 0.3	6.10 ± 0.4	5.50 ± 0.4	4.28 ± 0.24
SS-4	7.9 ± 0.3	0.01 ± 0.001	10.2 ± 0.2	8337.1 ± 1.2	242.6 ± 2.4	143.1 ± 0.6	6.9 ± 0.3	11.4 ± 0.2	4.57 ± 0.4	1.56 ± 0.2	0.09 ± 0.03
SS-5	24.8 ± 0.4	0.12 ± 0.001	28.8 ± 0.32	9963.6 ± 1.8	831.4 ± 2.3	274.5 ± 0.5	27.4 ± 0.42	31.3 ± 0.22	10.23 ± 0.21	5.16 ± 0.3	0.08 ± 0.02
SS-6	39.6 ± 0.55	0.03 ± 0.01	23.6 ± 0.24	9999.5 ± 1.9	888.9 ± 2.5	389.1 ± 0.44	71.3 ± 0.45	36.1 ± 0.24	8.07 ± 0.4	4.37 ± 0.2	0.06 ± 0.01
SS-7	75.7 ± 0.17	0.11 ± 0.01	26.3 ± 0.23	10116.3 ± 1.5	994.3 ± 1.8	823.9 ± 0.48	159.7 ± 0.58	39.3 ± 0.23	6.23 ± 0.5	5.33 ± 0.2	0.02 ± 0.01
SS-8	41.5 ± 0.87	0.04 ± 0.01	44.3 ± 0.45	10273.4 ± 1.2	1335.7 ± 3.3	2233.4 ± 1.2	114.1 ± 00.3	73.2 ± 0.32	14.14 ± 0.4	13.62 ± 0.3	0.08 ± 0.01
SS-9	78.3 ± 0.2	0.21 ± 0.1	37.1 ± 0.46	10052.4 ± 1.12	1318.0 ± 3.5	1164.1 ± 1.22	172.9 ± 0.2	39.8 ± 0.12	7.98 ± 0.5	5.85 ± 0.5	0.10 ± 0.01
SS-10	122.8 ± 0.23	0.41 ± 0.02	103.2 ± 0.45	10400.6 ± 0.89	3336.3 ± 3.4	1169.4 ± 1.1	232.4 ± 0.5	50.8 ± 0.14	7.64 ± 0.6	5.20 ± 0.4	0.08 ± 0.01
SS-11	32.3 ± 0.31	0.02 ± 0.01	41.6 ± 0.56	9930.6 ± 0.88	1281.8 ± 1.2	310.5 ± .9	102.1 ± 0.8	53.6 ± .3	16.59 ± .2	6.20 ± 0.2	0.05 ± 0.01
Min	7.9 ± 0.3	0.01 ± 0.001	10.2 ± 0.2	8337.1 ± 1.2	242.6 ± 2.4	143.1 ± 0.6	6.9 ± 0.3	11.4 ± 0.2	4.57 ± 0.4	1.56 ± 0.2	0.02 ± 0.01
Max	137.6 ± 0.6	1.76 ± 0.22	103.2 ± 0.45	10416.5 ± 1.4	3336.3 ± 3.4	2233.4 ± 1.2	367.9 ± 0.3	85.7 ± 0.4	16.59 ± .2	13.62 ± 0.3	4.28 ± 0.24
Mean	66.3 ± 83.2	0.54 ± 1.5	41.6 ± 53.7	9917 ± 1164.9	1170.5 ± 1573.2	901.3 ± 1221.4	143.5 ± 219.02	42.7 ± 44.03	9.59 ± 7.6	5.53 ± 5.9	0.49 ± 2.5
Standard Value[a,b]	22.8[b]	0.11[a,b]	77.2[a]	27,000[a]	1.17[b]	95[b]	33.0[b]	56.1[a]	-	-	-
Background Value[c]	13	0.2	100	50,000	950	70	55	75	25	1.8	0.07
World Average[d]	10.2	0.06	20.2	52,000	1100	10.3	20	40	10.4	-	-
World Normal[e]	19.0	3.00	100	26000	550	60	100	50	50	7.20	-
TRV[f]	31	0.6	26	-	120	-	16	16	-	6	-
SEL[g]	250	10	110	-	270	-	110	75	-	33	-
PEL[h]	91	3.5	90	-	-	-	197	36	-	17	-

[a] IAEA (1990) [131], [b]GESAMP (1982) [132], [c]Krauskopf & Bird (1995) [58], [d]Cox (1989) [133] & Iwegbue (2018) [134], [e]Bhuiyan et al., (2010) [39], [f]Toxicity Referency Value (TRV) by USEPA (1999) [135], [g]Severe Effect Level (SEL) & [h]Probable Effect Level (PEL) by MacDonald et al., (2000) [83].

laboratory analysis. The sediment quality parameters listed above were used to evaluate the taken triplicate samples from every sampling site, with the average values from each point included into the final result. The results are shown in Table 1. Results from three independent measurements at each sample location all showed RSDs of less than 10%.

As a way to ascertain the majority of the elements, AAS (atomic absorption spectrometer) analysis was used (Model: AA240FS, Varian, Australia). However, a Zeeman AAS (Model: GTA 120-AA240Z, Varian, Australia) was used to assess the concentration of Cd in sediment samples, and an AAS (Model: SpcetrAA 220 with ETC-60 and VGA-77, Varian, Australia) was used to estimate the concentration of As. This calibration curve was used to get an estimate of the sample's elemental content. For each element, working standard solutions at varying concentrations were produced by diluting CRM with deionized water, and their absorbances were measured against a calibration curve of concentration in comparison with absorbance. Sometimes, samples were diluted for components found at higher concentrations. Every instrumental calculation with RSD of below 5% was recorded as the mean of three consecutive duplicate measurements. Both the reference material's predicted value and its observed value fell within a 5–10% margin of error during analysis. Spike recovery (%) for all components was between 90% and 110% of the awaited values, as indicated by the equation below, confirming the precision and accuracy of the instrumental analysis using standard reference materials [28,45,54].

$$\text{Recovery}(\%) = \frac{(Concentration\ \ of\ \ spike\ \ sample - Concentration\ \ of\ \ unspike\ \ sample) \times 100}{Amount\ \ of\ \ spike}$$

To ensure analytical quality control, we used CRM (Fluka Analytical, Sigma-Aldrich, Germany) traceable to the National Institute of Standards and Technology (NIST), USA, at concentrations of 1000 ± 4 mg L-1. By recovering from spikes, the analytical method's validity was further supported. Replicate analysis was used to compare the analytical results to NIST traceable CRM, ensuring the accuracy and precision of the findings. Moreover, a blank for the reagent technique and standard solution were established after five and ten samples, accordingly.

2.4. Indexes for assessing sediment contamination

2.4.1. Enrichment factor (EF)

Differentiating between elements produced by natural weathering and those produced by human activity is an essential component of geochemical investigations. One extensively used method is normalization, which compares element concentrations to the composition or textural properties of the sediment [28,45]. Hence, the enrichment factor was determined by adjusting the element concentrations found in more than the average level of contamination [56]. According to Strbac et al., 2018 [57], it is important to consider the geochemical background values when establishing the quality criteria of soil and sediment and according to Sadanandan et al., 2023 [27], researchers use the average crustal abundance data as the background for the local interpretation of geochemical data. Therefore, as a point of reference, the average crustal abundance data were utilized from Krauskopf and Bird (1995) [58], and Fe was used to compute EF. Since its contribution comes almost exclusively from natural sources (98%) Fe was chosen as the standardizing element [59]. In fluvial and coastal sediments, Fe acts as both a substantial trace metal sorbent phase and a quasi-conservative tracer of the naturally occurring metal-bearing phases [3,60].

As calculated by Aprile and Bouvy (2008) [61], the enrichment factor (EF) for the concentration of trace metals in sediment is as follows:

$$\text{EF} = \frac{\left(\frac{X}{Fe}\right) Sediment}{\left(\frac{X}{Fe}\right) Background}$$

Where X stands for the trace metal being studied and X/Fe is the ratio of X's concentration to that of iron. If the EF of an element is between 0.05 and 1.5, it is almost certainly of natural or crustal origin [62]. For the components under consideration, the contamination level based on EF can be categorized into four categories [45,63] which is shown in a table (Table S1, Supplementary information).

2.4.2. Geo-accumulation index (Igeo)

Muller [64] introduced the geo-accumulation index in 1969, and its usage in determining elemental contamination in sediments has become widespread which was calculated by the following equation [65].

$$\text{Igeo} = \log_2 \left\{ \frac{C_{Trace\ \ metal}}{(1.5 \times C_{Background})} \right\}$$

Where C background is the metal's geochemical background concentration and $C_{Tracemetal}$ is the trace metal concentration in the sediment sample. Krauskopf and Bird's (1995) [58] data on crustal abundance were used as a baseline concentration. The correction factor of 1.5 is used to account for the possibility of changes in the background or control values owing to its possible terrigenous impacts [66].

The results of Igeo can be classified into seven grades or classes of sediment contamination [28,39,45,67] which is shown in a table (Table S1, Supplementary information).

2.4.3. Contamination factor (CF)

Each and every one trace metal in the sediment was evaluated for its ability to contribute to pollution using the contamination factor, which was computed by the following formula [28,45,68].

$$\text{CF} = \frac{C_{Trace\ \ metal}}{C_{Background}} \quad (3)$$

The background value is $C_{Bacground}$, and the statistics on crustal abundance from Krauskopf and Bird (1995) [58] were utilized in this context as background information. Sediment contamination levels in the current experiment were divided into four groups according to CF [69,70] (Table S1, Supplementary information).

2.4.4. Pollution load index (PLI)

To assess the overall extent of trace metal pollution in the sediment, pollution load index (PLI) was calculated [71] representing the geometric mean value of the contamination factors (CF) for the respective trace metals examined in this study.

$$\text{PLI} = (\text{CF1} \times \text{CF2} \times \text{CF3}\ldots\ldots\ldots\ldots\ldots \times \text{CFn})1/n$$

Where, n represents the number of examined trace metals. Results of PLI > 1 specifies the polluted sediment while PLI < 1 specifies no pollution [45,72].

2.4.5. Nemerow integrated pollution index (NIPI)

Furthermore, the gross pollution integrity of the studied ecosystem was appraised by the Nemerow Integrated Pollution Index (NIPI) [71,

72] [73,74]. The primary step in NIPI estimation was to develop a pollution index (PI). Similar to CF, the formula for PI involves averaging the concentration of metals over a certain number of sampling sites (often five). The formula of PI has been narrated earlier by Yu et al. (2004) [75] and Yang et al. (2011) [76], and it has been substantially implemented by Jiang et al. (2014) [77] and Al Anbari et al. (2015) [78].

$$\mathrm{PI} = \frac{Concentration \quad of \quad individual \quad trace \quad metal}{Background \quad value}$$

Anyway, the NIPI was evaluated by the equation below:

$$\mathrm{NIPI} = \sqrt{\frac{PI^2{}_{mean} + PI^2{}_{Maximum}}{2}}$$

Where, PI_{mean} is the average value of PI of individual trace metals and $PI_{Maximum}$ is the maximum value of PI of individual trace metals. The result of NIPI was categorized based on Cheng et al. [79] classification (Table S1, Supplementary information).

2.4.6. Toxic unit (TU) analysis

Relative toxic units (RTUs) are used to calculate the possible severe toxicity of trace metals in sediments. Toxic unit analysis measures how dangerous an environment is according to the concentration of potentially harmful substances in sediment [80]. When the sum of the toxic units for all sediment samples is greater than 4, the sediment's hazardous component's toxicity is still moderate to high [81,82]. The TUs were evaluated by the following formula for each metal:

$$\mathrm{TU} = \frac{C_{Trace \quad metal}}{PEL}$$

Where, $C_{Trace\ metal}$ is the trace metal concentration in sediment and PEL is the potential effect levels of trace metals in sediment. According to MacDonald et al., (2000) [83], the PEL values of Pb, Cd, Cr, Cu, Ni and As are 91, 3.5, 90, 197, 36 and 17, respectively.

$$\sum \mathrm{TU} = \mathrm{TU_{metal1}} + \mathrm{TU_{metal2}} + \mathrm{TU_{metal3}} + \ldots\ldots\ldots\ldots\ldots\ldots + \mathrm{TU_{metaln}}$$

Where, $\sum$TUs is the product of toxic units for trace metals in sediments [82].

2.4.7. Ecological risk factor (Er)

Ecological risk was introduced by Hakanson (1980) [68] and quantified by the following equation to quantify the possible ecological impact of a single trace metal contaminant:

$$\mathrm{Er} = \mathrm{Tf} \times \mathrm{CF}$$

Here, Tf stands for the corresponding trace metal's toxic reaction and CF for contamination factor. Lead, Cd, Cr, As, Mn, Ni, Cu, and Zn were the trace metals under study; their hazardous response factors were calculated as 5, 30, 2, 10, 1, 5, 5, and 1, accordingly [45,68] (Table S1, Supplementary information).

2.4.8. Potential ecological risk index (RI)

The potential ecological risk index is an improved version of the ecological risk factor that may be used to measure the impact that harmful compounds in sediments have on the ecosystem [84,85]. Here we illustrate the whole of the dangers posed by the trace metals in the sediment samples we tested [45,68].

$$\mathrm{RI} = \sum_{n=8}^{n} Er$$

RI was assessed for 8 (n = 8) trace metals and according to Jiao et al. (2015) [85] the index can be classified into four classes (Table S1, Supplementary information).

2.5. Human health risk evaluation

Health risk evaluation is a helpful method originated to appraise the probable harm that pollution poses to individuals [86]. As a first step, it is necessary to conduct an exposure assessment to distinguish between carcinogens and non-carcinogens and their respective dangers to the health of adults and children.

2.5.1. Exposure assessment

The purpose of an exposure assessment is to determine the level, frequency, and duration of a person's contact with environmental pollutants [87]. Trace metals may be ingested, inhaled, or absorbed via the skin when people come into touch with dust particles that have settled on sediments [86,88–92]. To calculate the chronic daily dose (CDD: mg/kg/day) of potentially harmful trace metals absorbed via each of the three routes of exposure, the following equations were utilized [88,93]:

$$CDD_{Ingestion} = \frac{C \times IngR \times EF \times ED}{BW \times AT} \times CF$$

$$CDD_{Inhalation} = \frac{C \times InhR \times EF \times ED}{PEF \times BW \times AT}$$

$$CDD_{Dermal} = \frac{C \times SA \times SL \times ABS \times EF \times ED}{BW \times AT} \times CF$$

where EF is the exposure frequency (days/year), ED is the exposure duration (year), C is the trace metal concentration in sediment (mg/kg), The skin's surface area (cm^2), SL is the adherence factor, and ABS is the dimensionless dermal absorption factor; According to USEPA (2002) [93,137] BW represents the average body weight (kg), AT denotes the average time (seconds), PEF represents the particle emission factor (m3/kg) (day), and CF represents the conversion factor (1 ×10–6 kg/mg). The relevant characteristics are shown in detail in a table (Table S2, Supplementary information). For the parameter values, the USEPA (2011) [94], De Miguel et al. (2007) [95], Wang et al. (2017) [96], and Bai et al. (2017) [97] were consulted.

2.5.2. Evaluation of non-carcinogenic risk

The hazard quotient (HQ), which is often used to describe the non-carcinogenic risk, is computed by dividing the chronic daily dose (CDD) of a given metal by the reference dose (RfD) [88]. The hazard index (HI) is the overall risk of non-carcinogenic trace metals by three routes of exposure for an individual trace metal [86]. Nevertheless, the following formulae are used to determine HQ and HI:

$$\mathrm{HQ} = \frac{CDD}{RfD}$$

$$\mathrm{HI} = \mathrm{HQ_{Ingestion}} + \mathrm{HQ_{Inhalation}} + \mathrm{HQ_{Dermal}}$$

Here, RfD is the reference dose (mg/kg/day) of every trace metal studied in this research. The reference doses (Rfd) of Pb, Cd, Cr, As, Mn, Fe, Co, Ni, Cu and Zn for ingestion pathway are 4×10^{-3}, 1×10^{-3}, 3×10^{-3}, 3×10^{-4}, 4.6×10^{-2}, 0.7, 2×10^{-2}, 2×10^{-2}, 4×10^{-2} and 3×10^{-1}, respectively; for inhalation pathway are 3.25×10^{-3}, 1×10^{-3}, 2.86×10^{-5}, 3.01×10^{-4}, 1.43×10^{-5}, 3×10^{-1}, 5.71×10^{-6}, 2.06×10^{-2}, 4.02×10^{-2} and 3×10^{-1}, respectively; and for dermal pathway are 5.25×10^{-4}, 1×10^{-5}, 6×10^{-5}, 1.23×10^{-4}, 1.84×10^{-3}, 0.14, 5.7×10^{-6}, 5.4×10^{-5}, 1.2×10^{-2} and 6×10^{-6}, respectively [98–104,138,139]. If the HQ or HI > 1, there may be potential non-carcinogenic effects on health, but HQ or HI ≤ 1 denotes there is no experience of any health risks for exposure by non-carcinogenic metals [88,94,105].

2.5.3. Carcinogenic risk assessment

With reference to carcinogenic risk, the incremental likelihood that a heavy metal user would get any sort of cancer from lifetime exposure

may be assessed [86,105,106]. According to the following calculation, the risk of cancer for an adult or kid may be calculated individually (USEPA, 1989, 2002) [88,93]:

$$CR = CDD \times SF$$

$$TCR = \sum CR$$

Where SF is the slope factor $(mg/kg/day)^{-1}$, CR is the carcinogenic risk (mg/kg/day), and TCR is the total carcinogenic risks. The slope factor of Pb, Cd, Cr, As and Ni for ingestion pathway are 8.5×10^{-3}, 0.38, 5.01×10^{-1}, 1.5 and 1.7, respectively; for inhalation pathway are 4.2×10^{-2}, 6.3, 0.42, 1.51×10^{1}, and 0.84, respectively; and for dermal pathway are 8.5×10^{-6}, 6.3, 2, 3.66 and 8.40×10^{1}, respectively [98–103,107].

2.5.4. Monte Carlo Simulation (MCS)

Since risk assessment involves evaluating potential risks based on known facts, personal characteristics, environmental variability, and lack of precision, uncertainty of risk is an inherent feature that needs to be considered [108–110]. To evaluate the carcinogenic and non-carcinogenic health hazards associated with exposure to trace metals contaminants, the Monte Carlo simulation technique has been appropriately used in this work utilizing the Oracle Crystal Ball (version 11.1.2.). The reduction of uncertainty is one of the benefits of the Monte Carlo simulation. To determine the probability distribution of risk, this method repeatedly selects arbitrary values from the probability distribution of a large number of input values [111–113]. Several numbers are used in the MCS instead of a single point value to perform multiple calculations and ultimately produce conclusions with varying assurance levels, ranging from 1% to 99%. The risks associated with the Hazard Index (HI) and incremental lifetime cancer risks (ILCR) are computed many times in the Monte Carlo simulation, using various random values for each input. Consequently, rather than having a single number, the output risk has a range of values. The impact of input factors on HI and ILCR values was ascertained using sensitivity analysis and likelihood of hazards. With a 95% confidence level and 100,000 iterations, the sensitivity analysis was predicted to guarantee numerical stability. This approach is often utilized in risk management practices and decision-making to pinpoint the primary causes of adverse health outcomes [114].

2.6. Statistical analysis

SPSS software (Version 20, IBM Corporation, Armonk, NY, USA) was used to further estimate the observed findings of the parameters of the sediment samples by statistical analysis. To ascertain the potential origin of trace metals (anthropogenic or natural), multivariate statistical analysis was used, such as principal component analysis (PCA) [55,72]; cluster analysis (CA) was used to categorize various geochemical groups [115]; Pearson's correlation matrix was used to determine the association among trace metals [116]. ArcGIS (10.8) software was used to create location map and spatial distribution maps. Moreover, lab origin pro-9 software employed to perform box plots and adobe Photoshop was used for the construction of graphical abstract. Microsoft Excel 2010 was frequently used for various analytical calculations.

3. Results and discussion

3.1. Trace metals concentration in sediment

The assessment of sediment samples from the ship breaking area of Bangladesh showed a variable distribution of several trace metals. The acquired results of trace metals with uncertainties are shown in Table 1. In addition, mean, median, 25–75% percentiles and the outliers of trace metals content in sediments are displayed in Fig. 3. The range of trace metals and their mean value in sediments was found as follows: 7.9 ± 0.3–137.6 ± 0.6 with an average 66.3 ± 83 for Pb, 0.01 ± 0.001–1.76 ± 0.2 with an average 0.54 ± 1.5 for Cd, 10.2 ± 0.2–103.2 ± 0.5 with an average 41.6 ± 54 for Cr, 8337.1 ± 1.2–10416.5 ± 1.4 with an average 9917 ± 1165 for Fe, 242.6 ± 2.4–3336.3 ± 3.4 with an average 1170.5 ± 1573 for Mn, 143.1 ± 0.6–2233.4 ± 1.2 with an average 901.3 ± 1221 for Zn, 6.9 ± 0.3–367.9 ± 0.3 with an average 143.5 ± 219 for Cu, 11.4 ± 0.2–85.7 ± 0.4 with an average 42.7 ± 44 for Ni, 4.57 ± 0.4–16.59 ± 0.2 with an average 9.59 ± 7.6 for Co, 1.56 ± 0.2–13.62 ± 0.3 with an average 5.53 ± 5.9 for As and 0.02 ± 0.01–4.28 ± 0.2 with an average 0.49 ± 2.5 for Ag.

3.2. Comparison of analyzed sediment data with standards

To estimate the level of trace metals, examined results of sediment samples were compared with standard, background and some reference values of unpolluted sediments. These findings were summarized in Table 1. The appraised Pb concentrations in sediment samples of almost all areas (except SS-4) were notably higher than the GESAMP standard, background, world average, world normal and toxicity reference (TRV) values. Although Pb concentration in sediments of some sampling sites highly exceeded the probable effect level (PEL), but average Pb concentration (66.3 mg/kg) was within the PEL and severe effect level (SEL). The mean Cd concentration (0.54 mg/kg) and Cd in sediments in most of the study areas was significantly higher than the IAEA, GESAMP standards, background, world average and TRV values. Average Cr concentration was higher than the world average and TRV values but lower than the IAEA standard, background, world normal, SEL and PEL values. Manganese concentrations in sediments from most of the sampling locations had surpassed the standard, background, world normal,

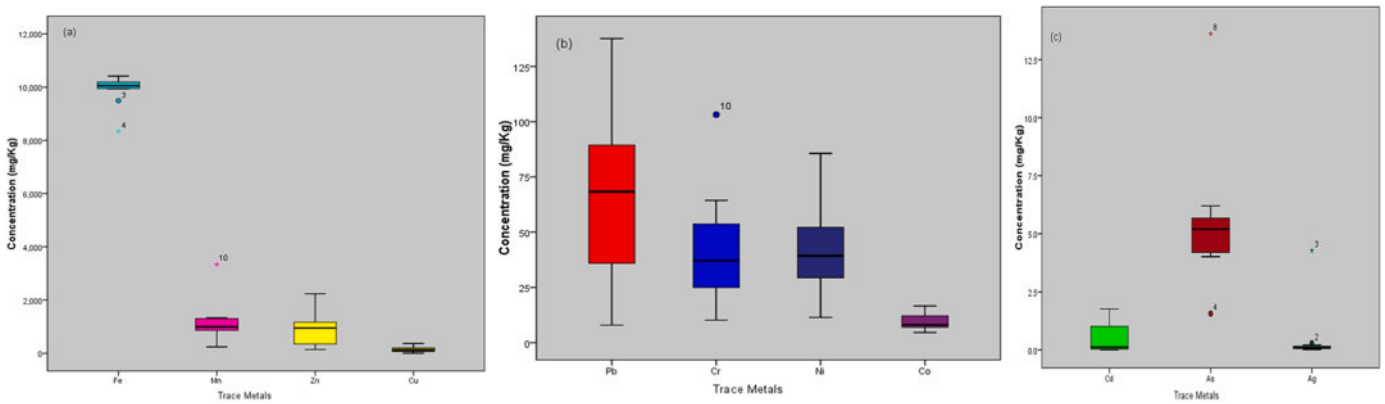

Fig. 3. Box plots of trace metals concentration in sediments of ship breaking area Bangladesh.

TRV, SEL values highly and mean Mn concentration was 1000 times higher than the GESAMP standard. Moreover, concentration of Zn of all sediment samples as well as its average value were 10–88 times greater than the standard, background, world average and world normal values. The concentration of Cu of most of the sediments and their mean results were higher than the standard, background, and reference values. Average Ni concentration was higher than the world average, TRV, PEL but lower than the standard, background, world normal, SEL values. In addition, average As and Ag concentrations were respectively 3 times and 7 times greater than the background value. However, Fe concentrations in sediments of every sampling point were within all standard, background and reference values.

3.3. Comparison of studied sediment data with reported data

The examined mean concentration of trace metals in sediments of the study area are compared with previous literature studies of Bangladesh and other top ranked ship breaking industrial Asian countries, which are shown in Table 2. Comparing our current study with the earlier two [3, 28] it can be designated that, although the Cd and Mn concentrations are higher than these studies, but content of Cr, Fe and Cu are lower. In addition to the concentrations of Pb, Ni and Zn of the present study are greater than the study of 2013 and lower than the study of 2020. This variation of trace metal concentration depends on some factors such as differences in sampling locations, seasonal variations and number of ships dismantled in the year etc. Beside these, the mean values of all and most of the trace metals of the current work are higher than the studies of Hossain et al., 2021 [19] and Rahman et al., 2019 [23], respectively. However, the toxic trace metal concentrations in the Alang-sosiya ship scrapping yard of India and the Aliaga ship breaking area of Turkey [117–120] are extremely higher in comparison with the Sitakunda ship breaking area of Bangladesh including present study (Table 2). Moreover, average Pb, Cd, Cr and Cu contents in sediments of highly impacted coastal zone of Karachi, Pakistan [121] are much higher than this work. But trace metal concentrations in sediments of southeast coast and west Bengal coast of India [122,123], northern Mediterranean coast of Turkey [124] and Karachi coast of Pakistan are lower than our current study.

3.4. Spatial distribution of trace metals in the study area

Spatial distribution maps are an extremely helpful tool for identifying hotspots with high concentrations of trace metals in the investigated regions and for differentiating between safe and risky zones [86, 91,92,125,126]. The spatial distribution maps of the examined trace metals in the ship breaking area of Bangladesh are shown in Fig. 4. These maps show locations with low, medium, and high concentrations of trace metals; the colors dark green, light green, yellow, brown, and red reflect these levels. The northern and southern regions of the research area are where high concentrations of Pb, Cr, Fe, Zn, Cu, Ni, and Co are found in spatial variations. In addition to these, high concentrations of Cd and Ag are found in the southern side while high Mn and As concentrations are in the northern side. However, the middle portion of the study area is comparatively safe zone. The ship breaking yards are irregularly situated along the coast of Sitakund, and large yards are situated in the northern and southern parts. These consistent spatial distribution patterns of trace metals suggest areas that might be impacted by the ship breaking industries in that region.

3.5. Assessment of trace metal pollution in sediment

In this research work a variety of indices were applied to estimate the pollution status of the Bangladesh's ship breaking areas sediments. Every one of these indices has a distinct interpretation and classification of the degree of contamination based on the chosen factors. For example, to determine the actual contribution from anthropogenic sources, enrichment factors (EF) for trace metals in specific sediment samples were calculated. In addition, trace metal accumulation with contamination loadings has been computed by the geo-accumulation index (Igeo). The results of EF and Igeo are shown in Fig. 5 and Table S3 (Supplementary information). In addition, spatial distribution maps of EF and Igeo values for studied trace metals in sediments are displayed in Fig. S1 (Supplementary information) and Fig. S2 (Supplementary information), respectively. The findings of EF values revealed that nearly all of the sediment samples were very severely enriched with Pb, Zn and As. Significant variations were observed in the EF values for Cd (0.30–46.39), Cu (0.75–32.11), and Ag (1.41–322.2), indicating diverse anthropogenic inputs. Beside these, most of the sediment samples were moderately to severely enriched with Mn and mild to moderately enriched with Ni, Cr and Co. According to the mean EF, concentrations of studied trace metals were found in the decreasing order as Zn (63.72) > Ag (36.15) > Pb (25.22) > As (15.31) > Cd (13.59) > Cu (12.82) > Mn (6.09) > Ni (2.83) > Cr (2.08) > Co (1.92). Spatial distribution maps of EF for Zn, Pb and As exhibit that sediments of the entire studied area is very severely polluted by these trace metals (except very small portion at SS-4 for Pb and As); for Ag and Cd southern zone has very severe sediment modification; for Cu sediments of both northern and southern sides are very severely polluted; and for Mn severe to very

Table 2
Comparison of average trace metal concentration of present data with the literature data of marine sediments of ship breaking areas of Bangladesh and other Asian countries.

Sample ID	Pb	Cd	Cr	Fe	Mn	Zn	Cu	Ni	Co	As	Ag	Reference
Ship Breaking area, Bangladesh	66.3	0.54	41.6	9917	1170.5	901.3	143.5	42.7	9.59	5.53	0.49	Present Study
Ship Breaking area, Bangladesh	61.9	-	30.8	-	586	76.6	45.9	32.3	-	-	-	[19]
Ship Breaking area, Bangladesh	68.3	0.49	64.6	93,015.1	1084.7	1226.3	255.4	54.2	-	-	-	[28]
Ship Breaking area, Bangladesh	90	-	11.9	68260	-	215.4	18.7	-	-	10.55	-	[23]
Ship Breaking area, Bangladesh	103.1	5.5	250.8	-	1002	713.3	180.2	90.8	-	-	-	[16]
Ship Breaking area, Bangladesh	18.09	0.24	658.45	58,959.1	938.27	355	189.18	32.64	21.73	6.81	-	[3]
Ship Breaking area, Bangladesh	55.94	-	106.8	-	20.09	70.72	50.09	-	-	-	-	[12]
Alang-Sosiya ship scrapping yard, India	169.98	32.7	290.18	137,990	4643.1	1222.18	214.41	172.53	52.55	-	-	[117]
Southeast coast of India	5.67	0.71	9.25	2779.81	54.84	14.19	3.55	6.43	-	-	-	[122]
West Bengal coast, eastern part of India	15.14	0.14	40.1	-	-	-	24.2	19.5	-	5.85	0.12	[123]
Aliaga Ship Breaking area, Turkey	368.75	2.85	147.25	54265	1256	1442.5	897.5	97.75	-	-	-	[118]
Heavily industrialized region in Turkey, including ship breaking yards.	128	0.88	30.6	23600	731	311	54.6	50.2	13.9	31.7	0.21	[120]
Aliaga ship recycling zone, Turkey	283.52	1.47	111.09	43641.47	551.20	605.43	320.95	98.67	-	-	-	[119]
Northern Mediterranean coast of Turkey	7.35	0.23	18.33	17061.43	198.32	44.81	6.12	30.95	6.21	19.58	-	[124]
Highly impacted coastal zone of Karachi, Pakistan	90.68	0.86	144.80	956.19	-	151.24	154.37	40.02	8.27	-	-	[121]
Karachi Coast, Pakistan	23.24	-	96.75	-	500	204.79	-	31.39	-	-	-	[136]

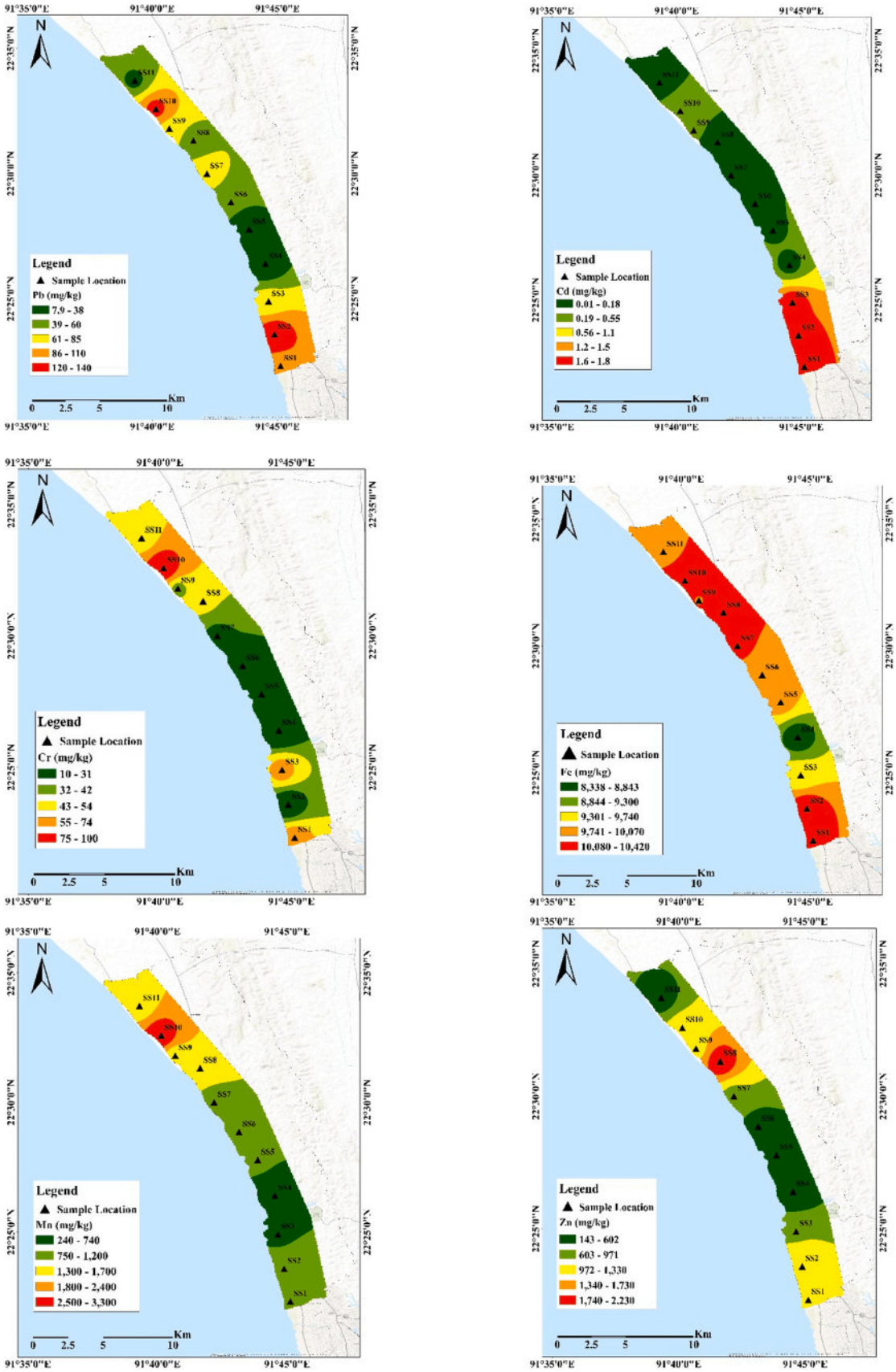

Fig. 4. Spatial distribution maps of Pb, Cd, Cr, Fe, Mn, Zn, Cu, Ni, Co, As and Ag concentrations in sediments of ship breaking area of Bangladesh.

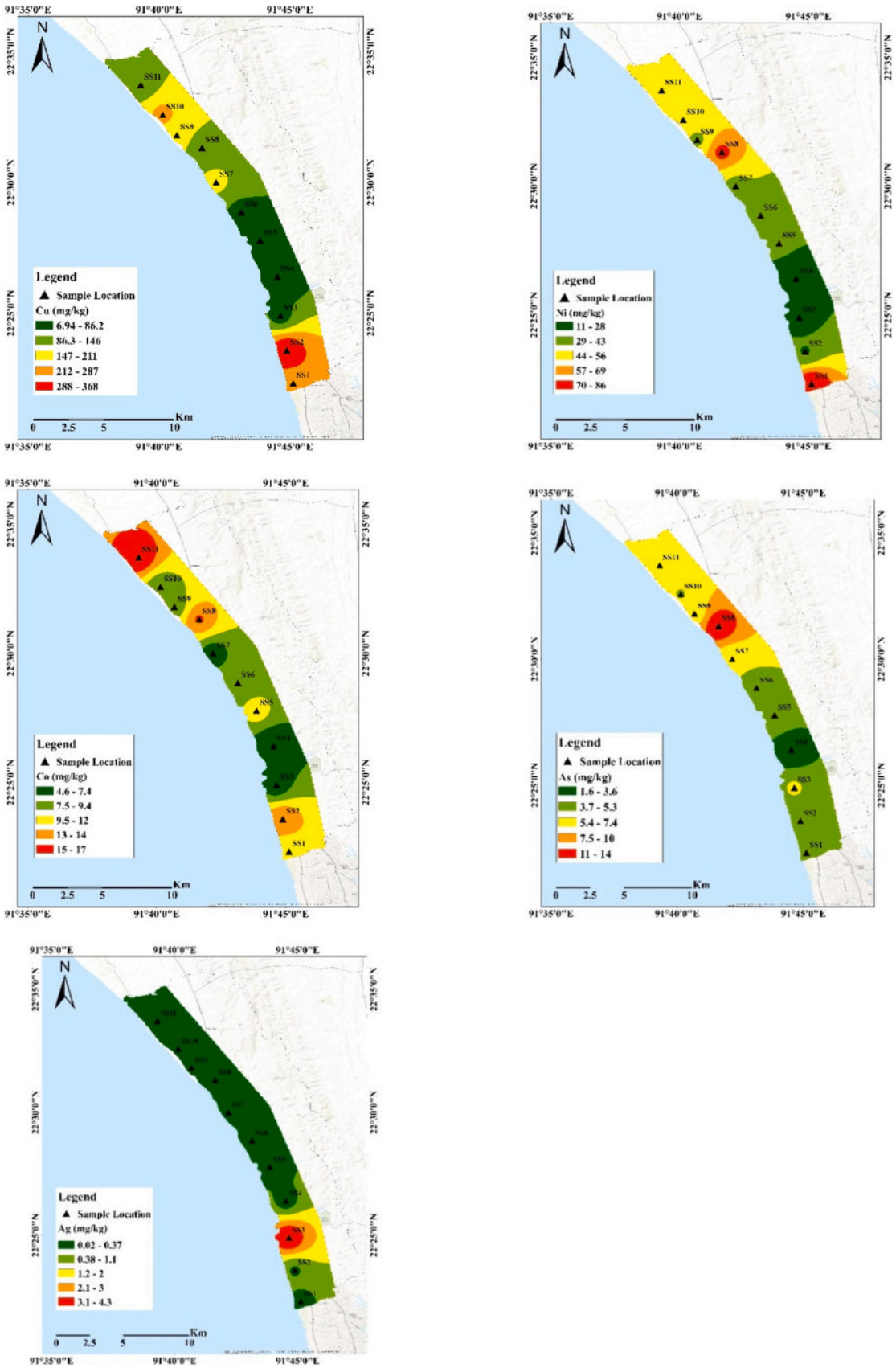

Fig. 4. (*continued*).

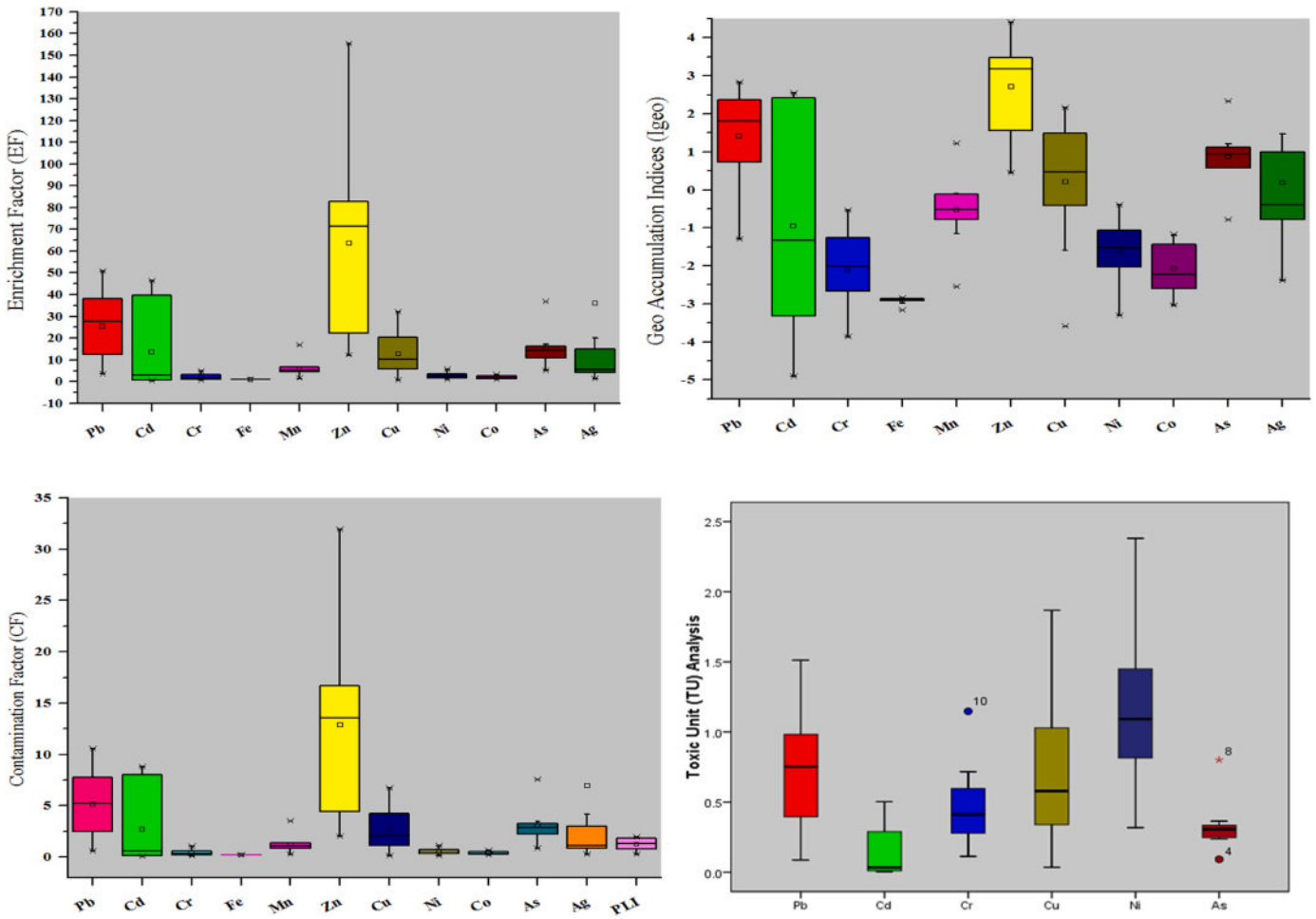

Fig. 5. Boxplots of Enrichment factor (EF), Geo-accumulation index (Igeo), Contamination factor (CF), Pollution load index (PLI) and Toxic unit (TU) analysis values of trace metals in sediments of ship breaking area, Bangladesh.

severe sediment contamination have found in a large portion of the northern side of the study area but no severe sediment modification has found for Ni, Cr and Co (Fig. S1, Supplementary information). Regarding Igeo 54.5% and 36.4% of sediment samples were accordingly heavily contaminated and moderately contaminated by Zn; sediments from almost all sampling sites were moderately to heavily contaminated by Pb and As (except SS-4); sediments from 63.6%, 36.4% and 27.3% of sampling sites were moderately to heavily contaminated by Cu, Cd and Ag, respectively. But all sites had negative Igeo values for Fe, Cr, Mn (except SS-10), Ni and Co that mean sediments were practically uncontaminated with these trace metals (Table S3, Supplementary information). The high EF and Igeo values for Zn, Pb, As, Cd, Cu, and Ag showed that these trace metals, which may have originated from both natural and man-made processes like ship scrapping, were heavily polluted in the sediments of the ship breaking region. Spatial variation maps of Igeo reveal that sediments of both northern and southern part of the study area are moderately to heavily contaminated for Pb and heavily to extremely contaminated for Zn; for Cd and Ag southern part while for As northern part are moderately to heavily contaminated by these metals; for Cu very small portion both in north and south part is moderately polluted. However, spatial maps of Igeo of sediments for Fe, Mn, Ni, Cr and Co depict that the whole study area (except very small portion near SS-10 for Mn) is practically uncontaminated by these metals (Fig. S2, Supplementary information).

Contamination factor (CF) analysis was executed to assess the contamination level of individual trace metal in sediments while pollution load index (PLI) was used to evaluate the overall pollution scenario of sediments from each sampling points. Moreover, nemerow integrated pollution index (NIPI) was also performed for the estimation of the comprehensive pollution integrity of the examined trace metals. The results of CF, PLI and NIPI are presented in Table S4 (Supplementary information). Considering CF values for Zn in almost all sediment samples showed very high contamination whereas, CF for Pb conveyed considerable to very high contamination of sediments in most of the sampling sites with large variation ranging from 0.61 to 10.59. The CF values for Cd in sediments from three sampling sites were very highly contaminated but sediments from rest of the sites had low to moderate contamination. Besides, CF for As and Cu in most of the sediment samples expressed moderate to considerable contamination. Although CF for Ag in two sampling points exhibited considerable to very high contamination but CF for Ag and Mn in majority of the samples indicated low to moderate contamination. However, the CF values of Fe, Cr, Ni and Co showed very low contamination level (Fig. 5). According to spatial variation maps produced by CF, the sediments in the study area's northern and southern parts have considerable to very high contamination with Pb and very high contamination with Zn. The southern part of the study area is very highly contaminated with Cd and Ag, while the northern part has considerable contamination with As. Small portion of the study area's north and south has considerable contamination with Cu. Although, the spatial distribution map of CF for Mn shows moderate contamination in the northern zone but the entire study area exhibit low contamination with Fe, Ni, Cr and Co (Fig. S3, Supplementary information). The PLI originated from CF revealed that 54.5% of the sampling sites had high pollution loads (PLI > 1). The results of PLI values

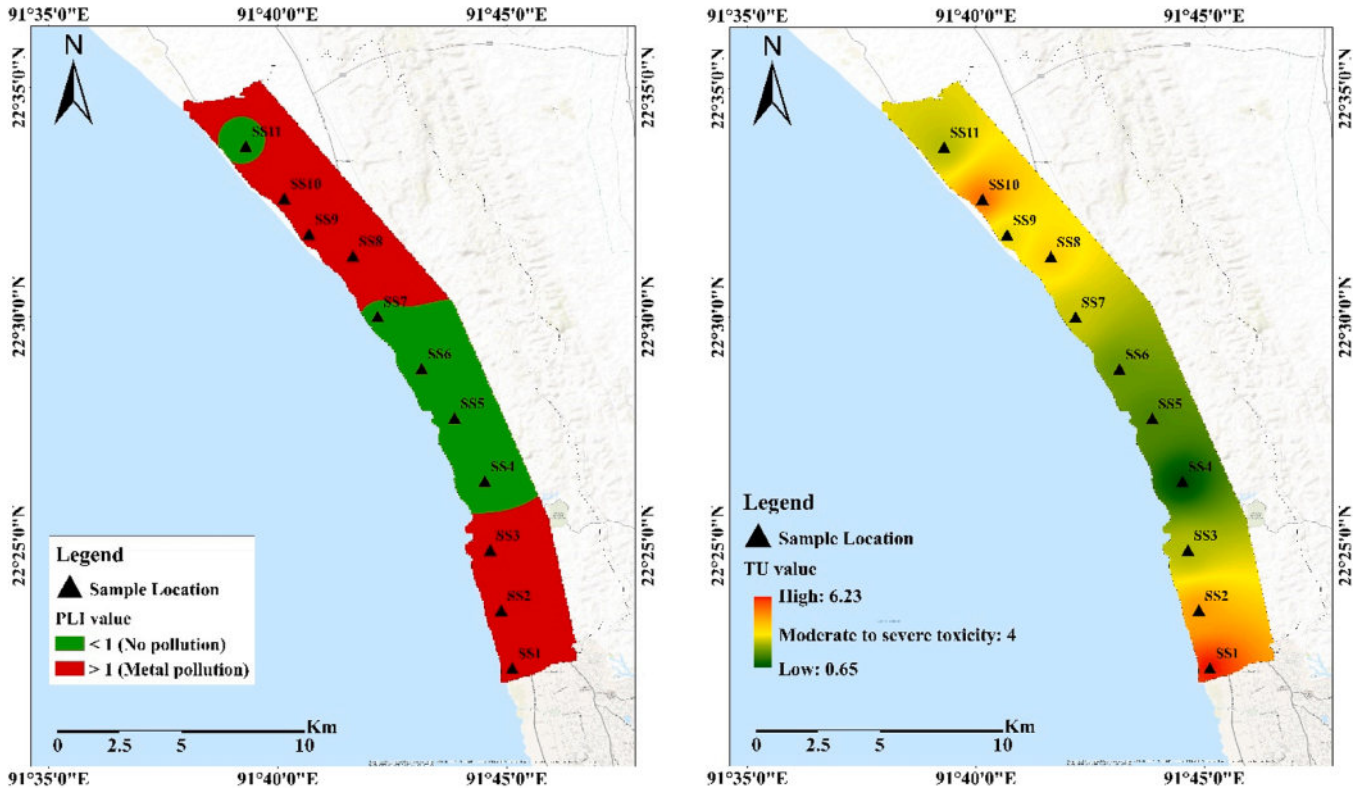

Fig. 6. Spatial distribution maps of PLI and ∑TU values in sediments of ship breaking area of Bangladesh.

for studied sampling locations followed the order of SS-1 > SS-2 > SS-3 > SS-10 > SS-9 > SS-8 > SS-7 > SS-11 > SS-5 > SS-6 > SS-4 (Table S4, Supplementary information). Spatial variation map of PLI shows that the northern and the southern sides of the study area are highly polluted by trace metals while the middle portion has no pollution (Fig. 6). However, based on the result of NIPI it can be shown that sediments of the study area were heavily polluted by Pb (8.31), Cd (6.51), Zn (24.33), As (5.78), Ag (43.52) and Cu (5.08) and moderately polluted by Mn (Table S1 and Table S4, Supplementary information).

Furthermore, toxic unit (TU) was also analyzed to estimate probable acute toxicity of trace metals in sediments. The results of toxic unit and sum of toxic unit (∑TUs) for trace metals are presented in Table S5 (Supplementary information) and Fig. 5. The average TU values of Pb, Cd, Cr, Cu, Ni and As in sediments were 0.729, 0.156, 0.462, 0.728, 1.186 and 0.325, respectively. According to the result of ∑TUs most of the sampling site's toxicity was moderate to high (∑TU>4). From the spatial distribution map of ∑TU it can be shown that both northern and southern zone of the study area have moderate to severe toxicity, but middle area has low toxicity (Fig. 6).

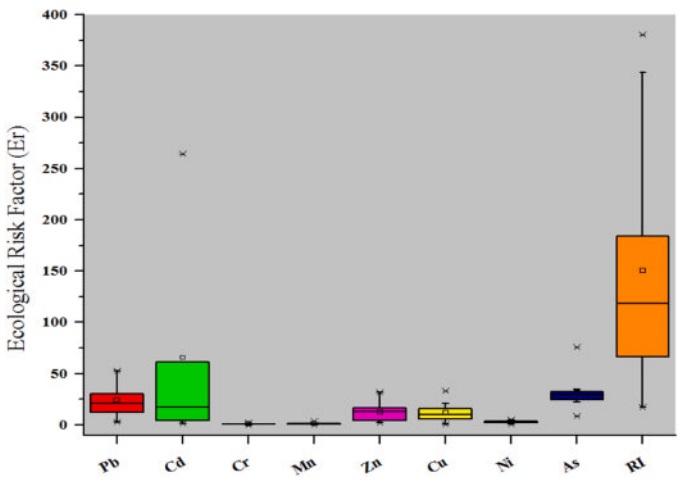

Fig. 7. Boxplots of ecological risk factor (Er) and potential ecological risk index (RI) values of trace metals in sediments of ship breaking area, Bangladesh.

3.6. Ecological risk

To evaluate the ecological concern of sediment pollution ecological risk factors (Er) for the eight environmentally toxic trace metals and to assess the sensitivity of the environment of these trace metals potential ecological risk (RI) for individual site has been calculated which are outlined in Fig. 7 and Table S6 (Supplementary information). In comparison with other studied trace metals Cd has the highest ecological risk with an average 81.6 in the study area which is likely due to cutting of ships as many parts of ships hold Cd. Beside this, Pb and As showed low to moderate potential ecological risk because Pb is used as a joining material of two metallic parts in ship building thus effluents of ship breaking painting of ships may increase the concentration of Pb in sediments [23]. However, the Er values of rest of the trace metals were found to be < 40 according to Hakanson (1980) [68] classification which means other studied trace metals have no risk to low potential ecological risk. The average Er values for each trace metals followed the order: Cd >As>Pb >Cu >Zn >Ni >Mn > Cr. According to the results of RI and RI classification of Jiao et al., 2015 [85] (Table S1) SS-1, SS-2, SS-3 sampling sites have significantly high potential ecological risk; SS-7, SS-8, SS-9, SS-10 sites have considerably high potential ecological risk; SS-5, SS-6, SS-11 sites have moderate potential ecological risk and SS-4 site has low potential ecological risk. The spatial distribution maps of Er of Cd and RI revealed the same pattern which demonstrates other studies [74,127,128] that means Cd contribution to potential ecological risk index of the environment is very significant [74]. Anyway, spatial maps show large portion of southern part have significantly high potential ecological risk as well as very high ecological risk by Cd (Fig. S4,

Supplementary information).

3.7. Health risk status

Working or living in an area where sediments were contaminated by toxic trace metals, human may be exposed to these metals through direct ingestion of sediment particles or foods (grown in contaminated sites), inhalation and dermal exposures, and face several health problems. As a result, the US EPA's (1989) [88] health risk assessment methodology was used to analyze the carcinogenic and non-carcinogenic health hazards of trace metals in sediments taken from the ship breaking area. The carcinogenic risk, hazard index (HI), hazard quotients (HQs), and chronic daily doses (CDDs) of the hazardous trace metals under study were evaluated for both adults and children to determine the health risk. Children are exposed to more harmful trace metals than adults are, according to the exposure scenario in this study, which showed that ingestion and dermal absorption are probably the predominant exposure pathways contributing significantly to the total risk outcomes.

3.7.1. Non-carcinogenic risk evaluation

The results of $HQ_{ingestion}$, HQ_{Dermal}, $HQ_{Inhalation}$ and HI from studied trace metals through all exposure pathways for children and adults are shown in Table 3 and the results of $CDD_{ingestion}$, CDD_{Dermal}, $CDD_{Inhalation}$ are presented in Table S7 (Supplementary information). Although, the $HQ_{ingestion}$ values of all studied metals for adults were lesser than the safe limits (< 1) but the maximum values of $HQ_{ingestion}$ of Pb (4.4×10^{-1}), Cr (4.4×10^{-1}), As (5.8×10^{-1}), Mn (9.3×10^{-1}), Fe (1.9×10^{-1}) and Cu (1.2×10^{-1}) for children were near the threshold limit. Similarly, except Zn, adults HQ_{Dermal} values were lesser while the maximum values of HQ_{Dermal} of Cr (1.14×10^{-1}), Mn (1.2×10^{-1}), Ni (1.05×10^{-1}) and Co (1.92×10^{-1}) for children were close to the threshold level. Surprisingly, HQ_{Dermal} values of Zn for adult (1.32) and children (9.91) were exceeded the safe limit (>1). However, the HI values of Zn for adults (ranges from 1.58 to 24.65 with an average 9.95) and for children (ranges from 0.21 to 3.3 with an average 1.33) were higher than the limit (>1), indicating that sediments of that area have a clear possible health risk by Zn. Plum et al. (2010) [129] reported that excessive Zn has been linked to adverse consequences including brain cell death, vomiting, and nausea, as well as Cu shortage. Even though, the maximum HI value of Mn (1.13) was greater than 1 and the maximum HI values of Pb (4.57×10^{-1}), Cr (5.55×10^{-1}), As (5.88×10^{-1}), Fe (1.95×10^{-1}), Cu (1.2×10^{-1}), Ni (1.59×10^{-1}) and Co (2.04×10^{-1}) for children were near the threshold value, but except Zn all HI values of trace metals for adults were less than the safe limit (< 1). That designates children are more susceptible than adults to the harmful effects of trace metals exposure via sediment. The order of estimated average HI values of examined trace metals in sediments for both adults and children was: Zn>Mn>As>Cr>Pb>Fe>Co>Ni>Cd (Table 3). The use of USEPA (1989) [88] parameters in this paper raises concerns about the suitability of the current approach for the population of Bangladesh, considering the disparities in exposure levels and age distributions. This has prompted concerns over the accuracy and reliability of the risk assessment estimates. In light of this, this work offers a preliminary risk assessment of human health, and going forward, more accurate evaluations for trace metals would be made.

3.7.2. Carcinogenic risk evaluation with Monte Carlo Simulation

The concept of carcinogenic risk pertains to the probability of an individual developing cancer over their lifespan due to exposure to various carcinogenic hazards [82,130]. The most toxic trace metals among the investigated parameters that pose a cancer risk are lead, Cd, Cr, As, and Ni. Therefore, in this study we only computed the increased cancer risks for both children and adults separately for Pb, Cd, Cr, As and Ni in the sediment for all potential routes and which are displayed in Table 4. According to USEPA (1989; 2002) [88,93], values of CR and TCR less than $1 \times 10 - 6$ should be considered inconsequential, values between $1 \times 10 - 6$ and $1 \times 10 - 4$ should be considered within the allowed range, and values beyond $1 \times 10 - 4$ should be considered

Table 3
Results of non-carcinogenic human health risks through ingestion, inhalation and dermal pathways for children and adults around the ship breaking area of Bangladesh.

Non-carcinogenic Risk		Children				Adults			
		$HQ_{ingestion}$	$HQ_{inhalation}$	HQ_{dermal}	**HI= ∑HQ**	$HQ_{ingestion}$	$HQ_{inhalation}$	HQ_{dermal}	**HI= ∑HQ**
Pb	Min	2.53×10^{-2}	8.68×10^{-7}	9.93×10^{-4}	2.62×10^{-2}	2.70×10^{-3}	4.90×10^{-7}	1.32×10^{-4}	2.84×10^{-3}
	Max	4.40×10^{-1}	1.51×10^{-5}	1.73×10^{-2}	4.57×10^{-1}	4.71×10^{-2}	8.53×10^{-6}	2.31×10^{-3}	4.94×10^{-2}
	Mean	2.12×10^{-1}	7.29×10^{-6}	8.33×10^{-3}	2.20×10^{-1}	2.27×10^{-2}	4.11×10^{-6}	1.11×10^{-3}	2.38×10^{-2}
Cd	Min	1.28×10^{-4}	3.57×10^{-9}	6.60×10^{-5}	1.94×10^{-4}	1.37×10^{-5}	2.01×10^{-9}	8.80×10^{-6}	2.25×10^{-5}
	Max	2.25×10^{-2}	6.29×10^{-7}	1.16×10^{-2}	3.41×10^{-2}	2.41×10^{-3}	3.55×10^{-7}	1.55×10^{-3}	3.96×10^{-3}
	Mean	6.90×10^{-3}	1.93×10^{-7}	3.56×10^{-3}	1.05×10^{-2}	7.40×10^{-4}	1.09×10^{-7}	4.75×10^{-4}	1.22×10^{-3}
Cr	Min	4.35×10^{-2}	1.27×10^{-4}	1.12×10^{-2}	5.48×10^{-2}	4.66×10^{-3}	7.18×10^{-5}	1.50×10^{-3}	6.23×10^{-3}
	Max	4.40×10^{-1}	1.29×10^{-3}	1.14×10^{-1}	5.55×10^{-1}	4.71×10^{-2}	7.27×10^{-4}	1.51×10^{-2}	6.30×10^{-2}
	Mean	1.77×10^{-1}	5.20×10^{-4}	4.57×10^{-2}	2.24×10^{-1}	1.90×10^{-2}	2.93×10^{-4}	6.10×10^{-3}	2.54×10^{-2}
As	Min	6.65×10^{-2}	1.85×10^{-6}	8.37×10^{-4}	6.73×10^{-2}	7.12×10^{-3}	1.04×10^{-6}	1.12×10^{-4}	7.24×10^{-3}
	Max	5.81×10^{-1}	1.62×10^{-5}	7.31×10^{-3}	5.88×10^{-1}	6.22×10^{-2}	9.12×10^{-6}	9.75×10^{-4}	6.32×10^{-2}
	Mean	2.36×10^{-1}	6.56×10^{-6}	2.97×10^{-3}	2.39×10^{-1}	2.53×10^{-2}	3.70×10^{-6}	3.96×10^{-4}	2.57×10^{-2}
Fe	Min	1.52×10^{-1}	1.00×10^{-5}	3.93×10^{-3}	1.56×10^{-1}	1.63×10^{-2}	1.00×10^{-5}	5.24×10^{-4}	1.68×10^{-2}
	Max	1.90×10^{-1}	1.00×10^{-5}	4.91×10^{-3}	1.95×10^{-1}	2.04×10^{-2}	1.00×10^{-5}	6.55×10^{-4}	2.10×10^{-2}
	Mean	1.81×10^{-1}	1.00×10^{-5}	4.67×10^{-3}	1.86×10^{-1}	1.94×10^{-2}	1.00×10^{-5}	6.24×10^{-4}	2.00×10^{-2}
Mn	Min	6.74×10^{-2}	6.06×10^{-3}	8.70×10^{-3}	8.22×10^{-2}	7.22×10^{-3}	3.42×10^{-3}	1.16×10^{-3}	1.18×10^{-2}
	Max	9.27×10^{-1}	8.34×10^{-2}	1.20×10^{-1}	1.13	9.94×10^{-2}	4.70×10^{-2}	1.60×10^{-2}	1.62×10^{-1}
	Mean	3.25×10^{-1}	2.92×10^{-2}	4.20×10^{-2}	3.97×10^{-1}	3.49×10^{-2}	1.65×10^{-2}	5.60×10^{-3}	5.69×10^{-2}
Zn	Min	6.10×10^{-3}	1.70×10^{-7}	1.57	1.580	6.53×10^{-4}	9.61×10^{-8}	0.21	2.11×10^{-1}
	Max	9.52×10^{-2}	2.66×10^{-6}	24.56	24.652	1.02×10^{-2}	1.50×10^{-6}	3.28	3.29
	Mean	3.84×10^{-2}	1.07×10^{-6}	9.91	9.949	4.12×10^{-3}	6.05×10^{-7}	1.32	1.33
Cu	Min	2.21×10^{-3}	6.13×10^{-8}	3.79×10^{-5}	2.24×10^{-3}	2.36×10^{-4}	3.46×10^{-8}	5.06×10^{-6}	2.41×10^{-4}
	Max	1.18×10^{-1}	3.27×10^{-6}	2.02×10^{-3}	1.20×10^{-1}	1.26×10^{-2}	1.84×10^{-6}	2.70×10^{-4}	1.29×10^{-2}
	Mean	4.59×10^{-2}	1.28×10^{-6}	7.89×10^{-4}	4.67×10^{-2}	4.91×10^{-3}	7.19×10^{-7}	1.05×10^{-4}	5.02×10^{-3}
Ni	Min	7.29×10^{-3}	1.98×10^{-7}	1.39×10^{-2}	2.12×10^{-2}	7.81×10^{-4}	1.11×10^{-7}	1.86×10^{-3}	2.64×10^{-3}
	Max	5.48×10^{-2}	1.49×10^{-6}	1.05×10^{-1}	1.59×10^{-1}	5.87×10^{-3}	8.38×10^{-7}	1.40×10^{-2}	1.98×10^{-2}
	Mean	2.73×10^{-2}	7.40×10^{-7}	5.22×10^{-2}	7.95×10^{-2}	2.93×10^{-3}	4.18×10^{-7}	6.96×10^{-3}	9.89×10^{-3}
Co	Min	2.92×10^{-3}	2.86×10^{-4}	5.29×10^{-2}	5.61×10^{-2}	3.13×10^{-4}	1.62×10^{-4}	7.06×10^{-3}	7.53×10^{-3}
	Max	1.06×10^{-2}	1.04×10^{-3}	1.92×10^{-1}	2.04×10^{-1}	1.14×10^{-3}	5.86×10^{-4}	2.56×10^{-2}	2.73×10^{-2}
	Mean	6.13×10^{-3}	6.01×10^{-4}	1.11×10^{-1}	1.18×10^{-1}	6.57×10^{-4}	3.39×10^{-4}	1.48×10^{-2}	1.58×10^{-2}

Table 4
Results of carcinogenic human health risks through ingestion, inhalation and dermal pathways for children and adults around the ship breaking area of Bangladesh.

Carcinogenic Risk		Children				Adults			
		$CR_{ingestion}$	$CR_{inhalation}$	CR_{dermal}	TCR= ∑CR	$CR_{ingestion}$	$CR_{inhalation}$	CR_{dermal}	TCR= ∑CR
Pb	Min	8.59×10^{-7}	1.19×10^{-10}	4.43×10^{-12}	8.59×10^{-7}	9.20×10^{-8}	6.68×10^{-11}	5.91×10^{-13}	9.21×10^{-8}
	Max	1.50×10^{-5}	2.06×10^{-9}	7.72×10^{-11}	1.50×10^{-5}	1.60×10^{-6}	1.16×10^{-9}	1.03×10^{-11}	1.60×10^{-6}
	Mean	7.21×10^{-6}	9.95×10^{-10}	3.72×10^{-11}	7.21×10^{-6}	7.72×10^{-7}	5.61×10^{-10}	4.96×10^{-12}	7.73×10^{-7}
Cd	Min	4.86×10^{-8}	2.25×10^{-11}	4.16×10^{-9}	5.28×10^{-8}	5.21×10^{-9}	1.27×10^{-11}	5.55×10^{-10}	5.77×10^{-9}
	Max	8.55×10^{-6}	3.96×10^{-9}	7.32×10^{-7}	9.29×10^{-6}	9.16×10^{-7}	2.23×10^{-9}	9.76×10^{-8}	1.02×10^{-6}
	Mean	2.62×10^{-6}	1.22×10^{-9}	2.24×10^{-7}	2.85×10^{-6}	2.81×10^{-7}	6.85×10^{-10}	2.99×10^{-8}	3.12×10^{-7}
Cr	Min	6.53×10^{-5}	1.53×10^{-9}	1.35×10^{-6}	6.67×10^{-5}	7.00×10^{-6}	8.63×10^{-10}	1.80×10^{-7}	7.18×10^{-6}
	Max	6.61×10^{-4}	1.55×10^{-8}	1.36×10^{-5}	6.75×10^{-4}	7.08×10^{-5}	8.73×10^{-9}	1.82×10^{-6}	7.27×10^{-5}
	Mean	2.66×10^{-4}	6.24×10^{-9}	5.49×10^{-6}	2.72×10^{-4}	2.86×10^{-5}	3.52×10^{-9}	7.32×10^{-7}	2.93×10^{-5}
As	Min	2.99×10^{-5}	8.42×10^{-9}	3.77×10^{-7}	3.03×10^{-5}	3.21×10^{-6}	4.75×10^{-9}	5.03×10^{-8}	3.26×10^{-6}
	Max	2.61×10^{-4}	7.35×10^{-8}	3.29×10^{-6}	2.65×10^{-4}	2.80×10^{-5}	4.14×10^{-8}	4.39×10^{-7}	2.85×10^{-5}
	Mean	1.06×10^{-4}	2.98×10^{-8}	1.34×10^{-6}	1.07×10^{-4}	1.14×10^{-5}	1.68×10^{-8}	1.78×10^{-7}	1.16×10^{-5}
Ni	Min	2.48×10^{-4}	3.42×10^{-9}	6.32×10^{-5}	3.11×10^{-4}	2.65×10^{-5}	1.93×10^{-9}	8.43×10^{-6}	3.50×10^{-5}
	Max	1.86×10^{-3}	2.57×10^{-8}	4.75×10^{-4}	2.34×10^{-3}	2.00×10^{-4}	1.45×10^{-8}	6.34×10^{-5}	2.63×10^{-4}
	Mean	9.28×10^{-4}	1.28×10^{-8}	2.37×10^{-4}	1.16×10^{-3}	9.94×10^{-5}	7.23×10^{-9}	3.16×10^{-5}	1.31×10^{-4}

potentially detrimental to human health. Although the mean $CR_{ingestion}$value for children of Pb (7.21×10^{-6}) and Cd (2.62×10^{-6}) were within the permissible limit but, the values of Cr (2.66×10^{-4}), As (1.06×10^{-4}) and Ni (9.28×10^{-4}) exceeded the maximum permissible limit. In addition, the mean CR_{Dermal} value of Ni (2.37×10^{-4}) was higher than the acceptable limit while the values of Cr (5.49×10^{-6}) and As (1.34×10^{-6}) were within the limit for children. Beside these, CR_{Dermal} value of Pb and Cd and all $CR_{Inhalation}$ values for children were negligible. The TCR values of Cr (2.72×10^{-4}), As (1.07×10^{-4}) and Ni (1.16×10^{-3}) for children were more than the allowable level but values of Pb (7.21×10^{-6}) and Cd (2.85×10^{-6}) were within the level. However, except the mean $CR_{ingestion}$ values of Cr (2.86×10^{-5}), As (1.14×10^{-5}), Ni (9.94×10^{-5}) and CR_{Dermal} value of Ni (3.16×10^{-5}), other $CR_{ingestion}$, CR_{Dermal} and all the $CR_{Inhalation}$ values for adults were negligible. For adult, the mean TCR values of Ni (1.31×10^{-4}) surpassed the acceptable level, Cr (2.93×10^{-5}) and As (1.16×10^{-5}) was within the level and the values of Pb (7.73×10^{-7}) and Cd (3.12×10^{-7}) were negligible, indicating that Ni, Cr and As may generate adverse cancer risks for worker's and local people of ship breaking area. The descending order of mean TCR values for both children and adults was: Ni> Cr> As> Pb> Cd. The above discussion stated that children are more vulnerable than adults and the ingestion and dermal absorption are the main pathways to the effects of adverse cancer risk. The spatial distribution maps of carcinogenic risk demonstrated that northern and southern parts were in high cancer risk for both adults and children with Pb, Cr, Ni and As but, with Cd southern parts was mainly in high risk (Fig. 8 and Fig. 9).

Due to the decreased representative variability of other elements, the Monte Carlo Simulation (MCS) was used for the hazard index (HI) and cancer risk (CR), considering the trace elements of As, Pb, Cr, Cd, and Ni, respectively (Fig. S5). For both the exposure duration and the 7-day frequency, the uncertainty of the risk estimate considered. According to Table 5, which displays the simulated findings, only two out of every 100,000 individuals working at the ship brake yard were at risk of developing cancer because of exposure to trace metals in the sediment, and even those two cases were completely below the permitted [16]. Fig. S5 (Supplementary information) and Table 5 display the outcomes including mean risk, standard deviation, 5th and 95th percentiles, base case, lowest and maximum values from the Monte Carlo simulation for the carcinogenic hazards. The carcinogenic risk mean value was found for the children and adults 2.02×10^{-4} and 2.08×10^{-4}. Whereas the maximum and minimum values were found to be 4.67×10^{-4}; 4.70×10^{-4} and 8.35×10^{-5}; 7.93×10^{-5}, respectively.

Utilizing the Monte Carlo Simulation (MCS) from the combined routes of ingestion, inhalation, and skin contact, the likelihood of cancer risk was calculated. 10000 trials were run via the simulation model. According to the simulation in Fig. S5 (Supplementary information), 5th and 95th percentile deterministic values were 1.37×10^{-4} and 2.75×10^{-4} for child and 1.47×10^{-4} and 2.78×10^{-4} for child adult respectively. It indicates that 95th percentile value is 2.01 and 1.89 times higher than 5th percentile deterministic values of child and adult values. Sensitivity analysis was used to determine which model input parameters were most crucial in terms of cancer risk, as Fig. S6 illustrates. From graph 2 of sensitivity chart (Fig. S6, Supplementary information), it is revealed that the positive effects of the exposure frequency (EF) in sediment samples was estimated as the significant factor for developing cancer (32%) for child and 31.2% for adult, followed by Ni concentration (4%), Expose Dose (ED) (0.0%), Cr concentration (0.7%), Mn concentration (0.5%) and As concentration (0.2%) for child while Ni concentration (2%), ED (0.2%), Cr concentration (0.6%), Fe concentration (0.4%) Co concentration (0.3%) and As concentration (0.1%) for adult. This is due to more contact with sediment to behavioral patterns. Furthermore, the recorded concentrations of Pb and Cd were found to be less than 0.01%, suggesting a negligible influence that may be disregarded. On the other hand, both child and adult, Body Weight (BW) (−64.7%) and Cu concentration (−4%) and Co concentration (−0.1%) for child and Mn concentration (−0.1%) showed negative effects on cancer risk estimation. According to the above results, long-term exposure of trace metals to the polluted sediment samples increased the likelihood of carcinogenic risk and the adverse effects in the ship-breaking yard workers.

3.8. Pollution source identification of trace metals

Using principal component analysis (PCA), cluster analysis (CA), and a Pearson correlation matrix, possible sources of trace metals were found. In this investigation, four principal components (PCs) with eigenvalues greater than 1 were recovered using PCA to examine the levels of contamination and the sources of trace metals. These PCs are shown in Table 6. The scree plot arranges eigenvalues in decreasing order based on the PC numbers, indicating the number of PCs used for dataset creation [2]. These components are then plotted in rotated space (Fig. S7, Supplementary information). The first component (PC1) depicted 40.58% of the total variance with strong positive loadings on Fe, Zn, Ni, Co and As having eigen value 4.46 and the third component (PC3) presented strong positive loadings between Cr and Mn experiencing 13.1% of the total variance with eigen value 1.44, and these components may be derived from both anthropogenic and natural sources. However, strong positive loadings were observed among Pb, Cd, Cu and Fe in PC2 and between Cd and Ag in PC4 possessing 20.99% and 12.25% of the total variance, respectively indicating anthropogenic source which is originated from ship breaking activities.

Moreover, to categorize the trace metals and sediment sample sites into different groups, hierarchical cluster analysis (CA) was carried out

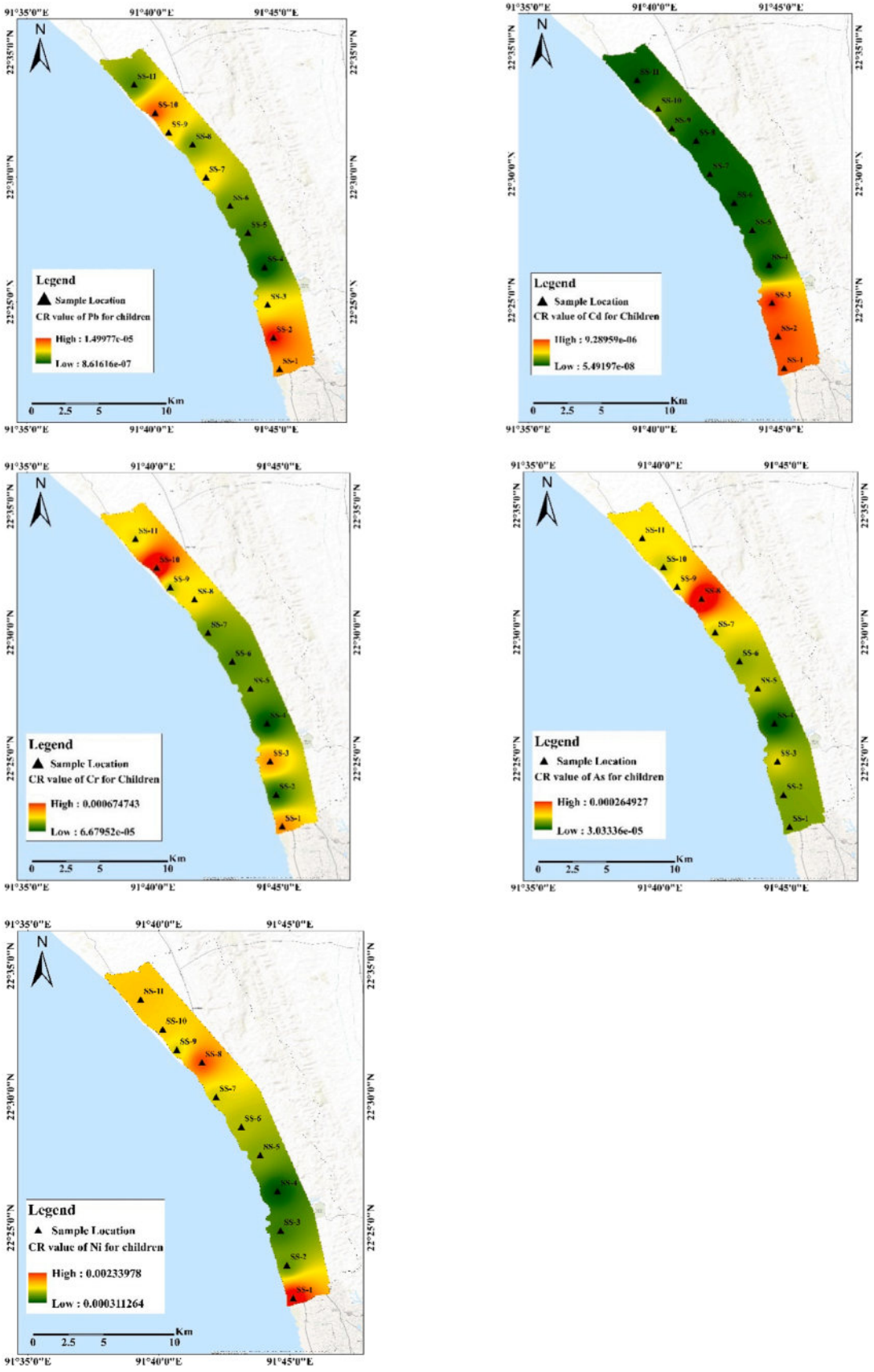

Fig. 8. Spatial distribution maps of carcinogenic risk (CR) of Pb, Cd, Cr, As, Ni for children from sediments of ship breaking area of Bangladesh.

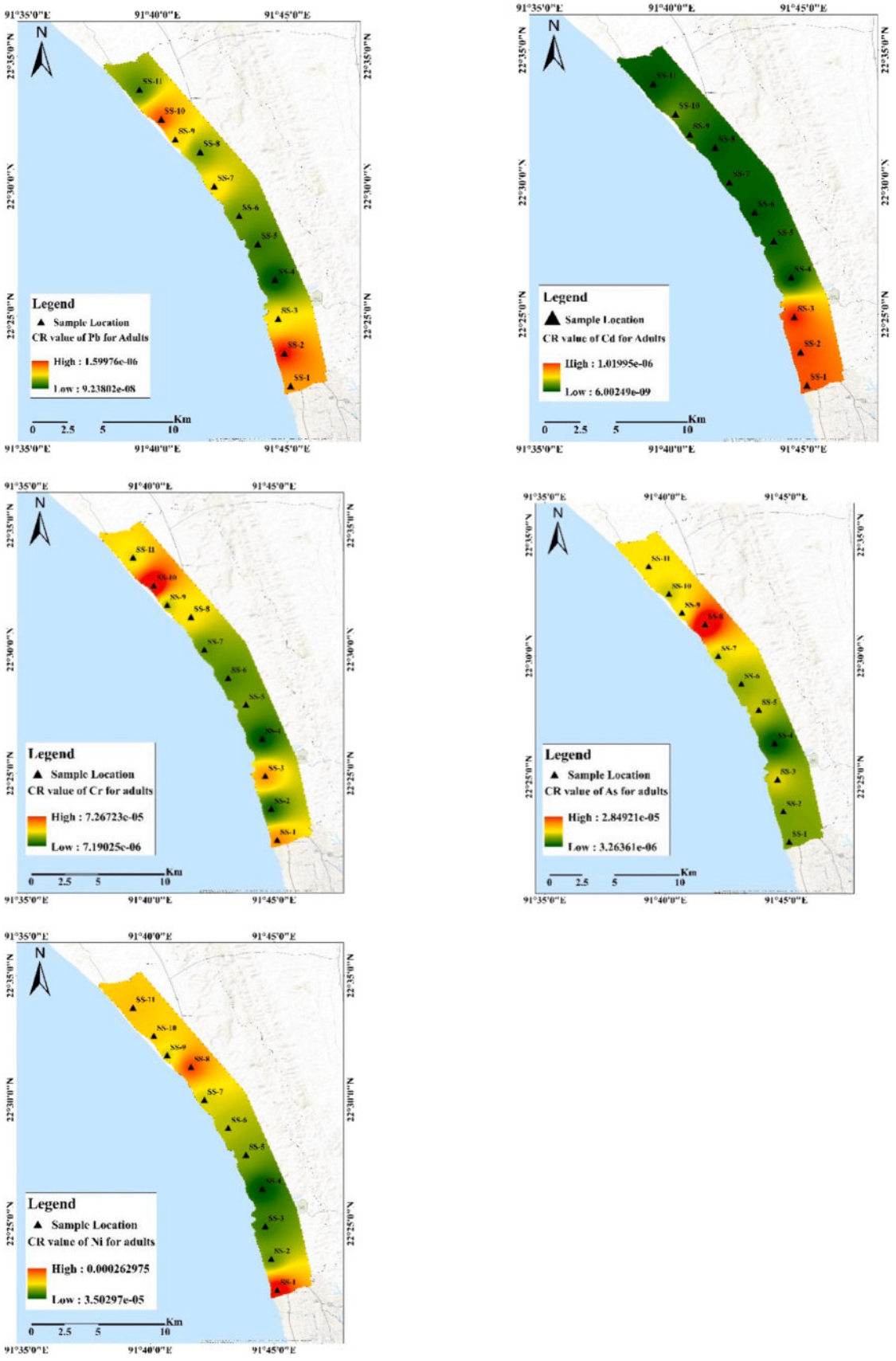

Fig. 9. Spatial distribution maps of carcinogenic risk (CR) of Pb, Cd, Cr, As, Ni for adults from sediments of ship breaking area of Bangladesh.

Table 5
Results of Monte Carlo simulation for carcinogenic risk assessment of both children and adults.

		Mean	SD	5th Percentile	95th Percentile	Base case	Max	Min
Children	$As_{ingestion}$	1.63E-05	4.40E-06	1.12E-05	2.20E-05	1.06E-04	3.70E-05	6.83E-06
	As_{dermal}	4.89E-15	2.24E-15	2.45E-15	8.04E-15	1.16E-10	1.84E-14	1.23E-15
	$As_{inhalation}$	9.37E-13	2.53E-13	6.47E-13	1.26E-12	1.52E-12	2.13E-12	3.97E-13
	$Cd_{ingestion}$	4.03E-07	1.18E-07	2.64E-07	5.59E-07	2.62E-06	9.61E-07	1.63E-07
	Cd_{dermal}	8.21E-16	0.00E+ 00	3.98E-16	1.37E-15	1.95E-11	3.43E-15	1.92E-16
	$Cd_{inhalation}$	3.81E-14	1.13E-14	2.51E-14	5.28E-14	6.21E-14	9.62E-14	1.51E-14
	$Cr_{ingestion}$	4.12E-05	1.14E-05	2.81E-05	5.64E-05	2.66E-04	1.01E-04	1.62E-05
	Cr_{dermal}	2.02E-14	9.43E-15	1.00E-14	3.27E-14	4.77E-10	8.64E-14	4.96E-15
	$Cr_{inhalation}$	1.97E-13	5.46E-14	1.35E-13	2.71E-13	3.19E-13	5.09E-13	7.98E-14
	$Pb_{ingestion}$	1.11E-06	3.01E-07	7.47E-07	1.50E-06	7.21E-06	2.69E-06	4.50E-07
	Pb_{dermal}	1.36E-16	0.00E+ 00	6.78E-17	2.19E-16	3.23E-12	5.79E-16	3.32E-17
	$Pb_{inhalation}$	3.12E-14	8.53E-15	2.12E-14	4.25E-14	5.08E-14	8.02E-14	1.31E-14
	$Ni_{ingestion}$	1.43E-04	3.92E-05	9.70E-05	1.95E-04	9.28E-04	3.28E-04	5.98E-05
	Ni_{dermal}	8.67E-13	3.99E-13	4.27E-13	1.41E-12	2.05E-08	3.49E-12	2.21E-13
	$Ni_{inhalation}$	4.03E-13	1.11E-13	2.74E-13	5.48E-13	6.55E-13	9.79E-13	1.71E-13
	Carcinogenic Risk Assessment	2.02E-04	5.50E-05	1.37E-04	2.75E-04	1.31E-03	4.67E-04	8.35E-05
Adults	$As_{ingestion}$	1.69E-05	4.47E-06	1.17E-05	2.25E-05	1.06E-04	4.14E-05	6.56E-06
	As_{dermal}	6.84E-16	0.00E+ 00	3.45E-16	1.09E-15	1.55E-11	1.93E-15	1.80E-16
	$As_{inhalation}$	9.68E-13	2.60E-13	6.68E-13	1.28E-12	1.52E-12	2.29E-12	3.78E-13
	$Cd_{ingestion}$	4.18E-07	1.19E-07	2.75E-07	5.72E-07	2.62E-06	9.27E-07	1.08E-07
	Cd_{dermal}	1.15E-16	0.00E+ 00	5.73E-17	1.91E-16	2.60E-12	3.47E-16	2.76E-17
	$Cd_{inhalation}$	3.95E-14	1.14E-14	2.63E-14	5.44E-14	6.21E-14	8.67E-14	1.02E-14
	$Cr_{ingestion}$	4.23E-05	1.11E-05	2.96E-05	5.68E-05	2.66E-04	9.80E-05	1.56E-05
	Cr_{dermal}	2.81E-15	1.26E-15	1.40E-15	4.46E-15	6.36E-11	8.44E-15	8.01E-16
	$Cr_{inhalation}$	2.02E-13	5.35E-14	1.40E-13	2.74E-13	3.19E-13	4.87E-13	7.51E-14
	$Pb_{ingestion}$	1.14E-06	3.03E-07	7.99E-07	1.55E-06	7.21E-06	2.73E-06	4.52E-07
	Pb_{dermal}	1.90E-17	0.00E+ 00	9.61E-18	3.05E-17	4.31E-13	5.48E-17	5.37E-18
	$Pb_{inhalation}$	3.23E-14	8.62E-15	2.23E-14	4.35E-14	5.08E-14	8.02E-14	1.28E-14
	$Ni_{ingestion}$	1.47E-04	3.87E-05	1.03E-04	1.97E-04	9.28E-04	3.34E-04	5.66E-05
	Ni_{dermal}	1.21E-13	5.45E-14	6.16E-14	1.94E-13	2.74E-09	3.73E-13	3.16E-14
	$Ni_{inhalation}$	4.15E-13	1.10E-13	2.89E-13	5.62E-13	6.55E-13	9.07E-13	1.60E-13
	Carcinogenic Risk Assessment	2.08E-04	5.41E-05	1.47E-04	2.78E-04	1.31E-03	4.70E-04	7.93E-05

Table 6
Varimax rotated principal component analysis of trace metals in the sediments of the ship breaking area of Bangladesh.

Parameters	Components			
	PC 1	PC 2	PC 3	PC 4
Pb	.055	**.914**	.355	.108
Cd	-.016	**.692**	-.089	**.678**
Cr	.161	.145	**.898**	.264
Fe	**.581**	**.538**	.319	-.232
Mn	.171	.256	**.869**	-.274
Zn	**.757**	.322	.240	.221
Cu	.200	**.953**	.130	-.114
Ni	**.703**	.173	.314	-.190
Co	**.719**	.217	-.246	-.285
As	**.923**	-.265	.150	.054
Ag	-.104	-.062	.034	**.959**
Eigenvalue	4.464	2.308	1.440	1.347
% of total variance	40.584	20.986	13.095	12.249
Cumulative % of variance	40.584	61.570	74.665	86.914

Every component belongs to rotated component matrix values of trace metals > 0.5

using Ward's approach and the findings are shown as Dendrogram (Fig. S8, Supplementary information). The Dendrogram of trace metals can be divided into four major clusters by setting the phenon line to a rescaled distance of roughly 10 to demonstrate statistical similarity. Lead and Cu were in Cluster 1, Cr and Mn were in Cluster 2, Zn, As, Fe, Ni, and Co were in Cluster 3, and Cd and Ag were in Cluster 4, all of which had positive loading on PC2, PC3, PC1, and PC4, respectively (Table 6).

Furthermore, to comprehend the coherence and connections of trace metals, Pearson correlation matrices were utilized, and the results are shown as heat map in Fig. 10. The correlations between trace metals were similar to the results of Cluster Analysis (CA) and Principal Component Analysis (PCA). Lead was strongly correlated with Cd, Cu

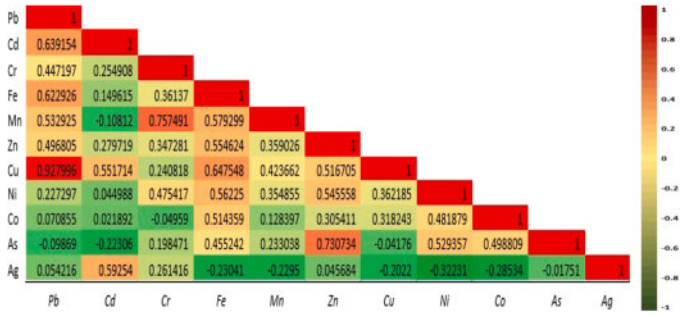

Fig. 10. Heat map of Pearson's correlation matrix among trace metals in sediments of the ship breaking area of Bangladesh.

and Fe, and Cd was significantly correlated with Ag, which support PC2 and PC4, respectively. The origin of these trace metals was same and which pinpoint the ship scrapping activities. However, rest of the trace metals are correlated with each other following PC1 and PC3 which may be originated from both anthropogenic and natural sources.

4. Conclusions

Sediment contamination levels with spatial distributions were assessed with their corresponding ecological and human health risks. Upon comparing the levels of studied trace metals in sediments with standards, we observed significant concentrations of Pb, Cd, Mn, Zn and Cu. According to spatial distribution maps these trace metals were mainly accumulated in the northern and southern portion of the study area rather than the middle portion. Varieties of pollution evaluation indices were applied to estimate the pollution status in sediments. The findings of EF and Igeo values revealed that nearly all ~~of~~ the sediment samples were very severely contaminated with Pb, Cd, Zn, Cu, As and Ag. Similarly, the result of NIPI also showed sediments of the study area

were heavily polluted by Pb, Cd, Zn, As, Ag and Cu. Considering CF values, most of the sediment samples were contaminated considerably to very highly by Pb, Zn, Cd, As and Cu and the PLI originated from CF revealed that 54.5% of the sampling sites had high pollution loads. Moreover, the total TU of six trace metals also disclosed that most of the sampling site's toxicity was moderate to high. The HI values of Zn for adults and children were higher than the safe limit, indicating that sediments of that area have a clear possible health risk by Zn. Although, for the children maximum HI value of Mn was greater than the safe limit and the maximum HI values of Pb, Cr, As, Fe, Cu, Ni and Co were near the threshold value, but except Zn all HI values for adults were less than this limit, designating children are more susceptible than adults to the harmful effects of trace metals exposure via sediment. The total carcinogenic risk values of Cr, As and Ni for children were greater than the allowable level and for adult, the mean TCR values of Ni surpassed the acceptable level but, Cr and As was within the level, designating Ni, Cr and As may generate adverse cancer risks for worker's and local people of ship breaking area. According to the Monte Carlo Simulation (MCS) among every 100,000 people active in ship braking yard, only 2 had the probability of the risk of getting cancer due to exposure to trace metals in ship braking yard's sediment which was entirely within the acceptable range. Principal component analysis, cluster analysis and Pearson correlation matrix disclosed that the origin of most of these trace metals were anthropogenic, attributing to ship breaking activities.

Sediments contaminated by trace metals will persist since ship breaking businesses are so prevalent and active in Bangladesh. Regular monitoring is thus crucial for managing the worrying situation. These interdisciplinary methods' findings will help us comprehend how trace metal contamination in sediments. This would further motivate planners and decision-makers to take the initiative for the proper control, regular monitoring, evaluation, and management of these trace metals emitted by the ship breaking activities to produce a healthy environment nearby. This investigation will also contribute to the body of knowledge in the relevant sectors and provide a benchmark for comparison with other ship-breaking regions across the globe. In addition to these, it will be useful for future scholars, academics, scientists, and environmentalists who will deal with the environmental compartments contaminated by ship breaking operations on a local and global scale.

Environmental Implication

Ship breaking industries are so prevalent in Bangladesh. Ships contain several hazardous materials like heavy metals. When ships are broken down, these substances can leach into the environment and posing severe health risks to workers and local communities. And, sediments contaminated by trace metals will persist since these industries are active. Thus, regular monitoring is crucial for managing the worrying situation. These interdisciplinary findings will help us to motivate planners and decision-makers to take the initiative for the proper monitoring and management of these trace metals emitted by the ship breaking activities in order to produce a healthy environment nearby.

Funding

The authors received no specific funding for this research work.

CRediT authorship contribution statement

Nahar Aynun: Data curation, Formal analysis, Investigation, Methodology, Resources, Visualization, Writing – review & editing. **Hasan Mehedi:** Data curation, Formal analysis, Investigation, Methodology, Resources, Validation, Visualization, Writing – review & editing. **Uddin Md. Ripaj:** Conceptualization, Formal analysis, Methodology, Software, Validation. **Zaman Mohammad Nazim:** Conceptualization, Formal analysis, Methodology, Validation, Visualization. **Hasan Asma Binta:** Conceptualization, Data curation, Formal analysis, Investigation, Methodology, Software, Validation, Writing – original draft. **Reza A.H.M. Selim:** Conceptualization, Formal analysis, Investigation, Methodology, Supervision, Validation, Writing – review & editing. **Siddique Md. Abu Bakar:** Conceptualization, Data curation, Formal analysis, Methodology, Resources, Supervision, Validation, Visualization, Writing – review & editing. **Akbor Md. Ahedul:** Data curation, Formal analysis, Methodology, Resources, Validation, Writing – review & editing. **Islam Iftekharul:** Conceptualization, Formal analysis, Methodology, Validation, Visualization.

Declaration of Competing Interest

The authors declare that they have no known competing financial interests or personal relationships that could have appeared to influence the work reported in this paper.

Data Availability

Data will be made available on request.

Acknowledgments

The authors are grateful to the authority of the Institute of National Analytical Research and Service (INARS), Bangladesh Council of Scientific and Industrial Research (BCSIR), Dhaka, Bangladesh for providing laboratory facilities and other logistic support during the research work.

Appendix A. Supporting information

Supplementary data associated with this article can be found in the online version at doi:10.1016/j.jhazmat.2023.133214.

References

[1] Talukder, M.I., Fakhruddin, A.N.M., Hossain, M.A., 2015. Environmental impacts of ship breaking and recycling industry of Sitakunda, Chittagong, Bangladesh. Adv Nat Sci 8, 51–58. https://doi.org/10.3968/6492.
[2] Hasan, A.B., Reza, A.H.M.S., Siddique, M.A.B., Akbor, M.A., Nahar, A., Hasan, M., et al., 2022. Spatial distribution, water quality, human health risk assessment, and origin of heavy metals in groundwater and seawater around the ship-breaking area of Bangladesh. Environ Sci Pollut Res 30, 16210–16235. https://doi.org/10.1007/s11356-022-23282-4.
[3] Hasan, A.B., Kabir, S., Selim Reza, A.H.M., Nazim Zaman, M., Ahsan, A., Rashid, M., 2013. Enrichment factor and geo-accumulation index of trace metals in sediments of the ship breaking area of Sitakund Upazilla (Bhatiary-Kumira), Chittagong, Bangladesh. J Geochem Explor 125, 130–137. https://doi.org/10.1016/j.gexplo.2012.12.002.
[4] Khan, R., Das, S., Kabir, S., Habib, M.A., Naher, K., Islam, M.A., et al., 2019. Evaluation of the elemental distribution in soil samples collected from ship-breaking areas and an adjacent island. J Environ Chem Eng 7, 103189. https://doi.org/10.1016/j.jece.2019.103189.
[5] Mathew, E., 2021. Ship recycling, market imperfections and the relevance of a consortium of ship recycling nations in the Indian subcontinent. J Int Marit Saf Environ Aff Shipp 5 (2), 23–31. https://doi.org/10.1080/25725084.2021.1921994.
[6] Ali, M.M., Islam, M.S., Islam, A.R.M.T., Bhuyan, M.S., Ahmed, A.S.S., Rahman, M. Z., et al., 2022. Toxic metal pollution and ecological risk assessment in water and sediment at ship breaking sites in the Bay of Bengal Coast, Bangladesh. Mar Pollut Bull 175, 113274. https://doi.org/10.1016/j.marpolbul.2021.113274.
[7] Ozturkoglu, Y., Kazancoglu, Y., Ozkan-Ozen, Y.D., 2019. A sustainable and preventative risk management model for ship recycling industry. J Clean Prod 238, 117907. https://doi.org/10.1016/j.jclepro.2019.117907.
[8] Barua, S., Rahman, I.M.M., Hossain, M.M., Begum, Z.A., Alam, I., Sawai, H., et al., 2018. Environmental hazards associated with open-beach breaking of end-of-life ships: a review. Environ Sci Pollut Res 25, 30880–30893. https://doi.org/10.1007/s11356-018-3159-8.
[9] Sujauddin, M., Koide, R., Komatsu, T., Hossain, M.M., Tokoro, C., Murakami, S., 2015. Characterization of ship breaking industry in Bangladesh. J Mater Cycles Waste Manag 17, 72–83. https://doi.org/10.1007/s10163-013-0224-8.
[10] Hossain, M.M., Islam, M.M., 2006. Ship breaking activities and its impact on the coastal zone of Chittagong, Bangladesh: towards sustainable management. Young Power in Social Action (YPSA),, Chittagong.

[11] OSHA, 2001. Shipbreaking fact sheet. U.S. Department of Labor, Occupational Safety and Health Administration, Washington, DC.
[12] Aktaruzzaman, M., Chowdhury, M.A.Z., Fardous, Z., Alam, M.K., Hossain, M.S., Fakhruddin, A.N.M., 2014. Ecological risk posed by heavy metals contamination of ship breaking yards in Bangladesh. Int J Environ Res 8, 469–478.
[13] Hossain, M.S., Fakhruddin, A.N.M., Chowdhury, M.A.Z., Gan, S.H., 2016. Impact of ship-breaking activities on the coastal environment of Bangladesh and a management system for its sustainability. Environ Sci Pol 60, 84–94.
[14] Rabbi, H.R., Rahman, A., 2017. Ship breaking and recycling industry of Bangladesh; issues and challenges. Procedia Eng 194, 254–259. https://doi.org/10.1016/j.proeng.2017.08.143.
[15] Sujauddin, M., Koide, R., Komatsu, T., Hossain, M.M., Tokoro, C., Murakami, S., 2017. Ship breaking and the steel industry in Bangladesh: a material flow perspective. J Ind Ecol 21, 191–203.
[16] Alam, I., Barua, S., Ishii, K., Mizutani, S., Hossain, M.M., Rahman, I.M.M., et al., 2019. Assessment of health risks associated with potentially toxic element contamination of soil by end-of-life ship dismantling in Bangladesh. Environ Sci Pollut Res 26, 24162–24175. https://doi.org/10.1007/s11356-019-05608-x.
[17] Mitra, N., Ahmad Shahriar, S., Lovely, N., Khan, S., Rak, A.E., Kar, S.P., et al., 2020. Assessing energy-based co2 emission and workers' health risks at the shipbreaking industries in bangladesh. Environ - MDPI 7. https://doi.org/10.3390/environments7050035.
[18] Pasha, M., Hasan, M.A., Rahman, I., Hasnat, A., 2012. Assessment of ship breaking and recycling industries in Bangladesh—an effective step towards the achievement of environmental sustainability. International Conference on Agricultural, Environmental and Biological; Sciences (ICAEBS' 2012).
[19] Hossain, M.B., Runu, U.H., Sarker, M.M., Hossain, M.K., Parvin, A., 2021. Vertical distribution and contamination assessment of heavy metals in sediment cores of ship breaking area of Bangladesh. Environ Geochem Health 43, 4235–4249. https://doi.org/10.1007/s10653-021-00919-w.
[20] Andersen, A.B., 2001. Worker safety in the ship-breaking industries. International Labour Office, Geneva. WP.167) (ISBN: 92–2–112464–9.
[21] Hasan, A.B., Kabir, S., Reza, A.H.M.S., Zaman, M.N., Ahsan, M.A., Akbor, M.A., et al., 2013. Trace metals pollution in sea water and groundwater in the ship breaking area of Sitakund Upazilla Chittagong, Bangladesh. Mar Pollut Bull 71 (1–2), 317–324.
[22] Islam, K.L., Hossain, M.M., 1986. Effect of ship scrapping activities on soil and sea environment in the coastal area of Chittagong, Bangladesh. Mar Pollut Bull 17 (10), 462–463.
[23] Rahman, M.S., Hossain, M.B., Babu, S.M.O.F., Rahman, M., Ahmed, A.S.S., Jolly, Y.N., et al., 2019. Source of metal contamination in sediment, their ecological risk, and phytoremediation ability of the studied mangrove plants in ship breaking area, Bangladesh. Mar Pollut Bull 141, 137–146. https://doi.org/10.1016/j.marpolbul.2019.02.032.
[24] Tokatli, C., Islam, M.S., 2022. Spatiotemporal variations and bio-geo-ecological risk assessment of heavy metals in sediments of a wetland of international importance in Turkey. Arab J Geosci. https://doi.org/10.1007/s12517-021-09227-0.
[25] Aydin, H., Tepe, Y., Ustaoglu, F., 2023. A holistic approach to the eco-geochemical risk assessment of trace elements in the estuarine sediments of the Southeastern Black Sea. Mar Pollut Bull 189, 114732. https://doi.org/10.1016/j.marpolbul.2023.114732.
[26] Kodat, M., Tepe, Y., 2023. A holistic approach to the assessment of heavy metal levels and associated risks in the coastal sediment of Giresun, southeast Black Sea. Heliyon 9, 16424. https://doi.org/10.1016/j.heliyon.2023.e16424.
[27] Sadanandan, H., Dharmalingam, S.N., Sridharan, M., Agarwal, N., Anbuselvan, N., 2023. Assessment of trace metal pollution in surface sediments from southwestern part of Bay of Bengal, India. J. Geol Soc India 99, 383–389. https://doi.org/10.1007/s12594-023-2321-1.
[28] Hasan, A.B., Reza, A.H.M.S., Kabir, S., Siddique, M.A.B., Ahsan, M.A., Akbor, M. A., 2020. Accumulation and distribution of heavy metals in soil and food crops around the ship breaking area in southern Bangladesh and associated health risk assessment. SN Appl Sci 2, 1–18. https://doi.org/10.1007/s42452-019-1933-y.
[29] Islam, M.S., Ahmed, M.K., Habibullah-Al-Mamun, M., Hoque, M.F., 2015. Preliminary assessment of heavy metal contamination in surface sediments from a river in Bangladesh. Environ Earth Sci 73, 1837–1848. https://doi.org/10.1007/s12665-014-3538-5.
[30] Raknuzzaman, M., Ahmed, M.K., Islam, M.S., Habibullah-Al-Mamun, M., Tokumura, M., Sekine, M., et al., 2016. Trace metal contamination in commercial fish and crustaceans collected from coastal area of Bangladesh and health risk assessment. Environ Sci Pollut Res 23, 17298–17310. https://doi.org/10.1007/s11356-016-6918-4.
[31] Yuan, G.L., Liu, C., Chen, L., Yang, Z., 2011. Inputting history of heavy metals into the inland lake recorded in sediment profiles: poyang Lake in China. J Hazard Mater 185, 336–345.
[32] Mitra, S., Chakraborty, A.J., Tareq, A.M., Emran, T.B., Nainu, F., Khusro, A., et al., 2022. Impact of heavy metals on the environment and human health: novel therapeutic insights to counter the toxicity. J King Saud Univ Sci 34, 101865. https://doi.org/10.1016/j.jksus.2022.101865.
[33] Bhuyan, M.S., Bakar, M.A., Akhtar, A., Hossain, M.B., Ali, M.M., Islam, M.S., 2017. Heavy metal contamination in surface water and sediment of the Meghna River, Bangladesh. Environ Nanotechnol Monit Manag 8, 273–279. https://doi.org/10.1016/j.enmm.2017.10.003.
[34] Ali, M.M., Ali, M.L., Islam, M.S., Rahman, M.Z., 2016. Preliminary assessment of heavy metals in water and sediment of Karnaphuli River, Bangladesh. Environ Nanotechnol Monit Manag 5, 27–35. https://doi.org/10.1016/j.enmm.2016.01.002.
[35] Kibria, G., Hossain, M.M., Mallick, D., Lau, T.C., Wu, R., 2016. Monitoring of metal pollution in waterways across Bangladesh and ecological and public health implications of pollution. Chemosphere 165, 1–9. https://doi.org/10.1016/j.chemosphere.2016.08.121.
[36] Kibria, G., Hossain, M.M., Mallick, D., Lau, T.C., Wu, R., 2016. Trace/heavy metal pollution monitoring in estuary and coastal area of the Bay of Bengal, Bangladesh and implicated impacts. Mar Pollut Bull 105, 93–402. https://doi.org/10.1016/j.marpolbul.2016.02.021.
[37] Roberts, D.A., 2012. Causes and ecological effects of resuspended contaminated sediments (RCS) in marine environments. Environ Int 40, 230–243.
[38] Tepe, Y., Simsek, A., Ustaoglu, F., Tas, B., 2022. Spatial–temporal distribution and pollution indices of heavy metals in the Turnasuyu Stream sediment,Turkey. Environ Monit Assess 194, 818. https://doi.org/10.1007/s10661-022-10490-1.
[39] Bhuiyan, M.A.H., Parvez, L., Islam, M.A., Dampare, S.B., Suzuki, S., 2010. Heavy metal pollution of coal mine-affected agricultural soils in the northern part of Bangladesh. J Hazard Mater 173, 384–392.
[40] Sahoo, P.K., Bhattacharyya, P., Tripathy, S., Equeenuddin, S.M., Panigrahi, M.K., 2010. Influence of different forms of acidities on soil microbiological properties and enzyme activities at an acid mine drainage contaminated site. J Hazard Mater 179, 966–975. https://doi.org/10.1016/j.jhazmat.2010.03.099.
[41] Halim, M.A., Majumder, R.K., Zaman, M.N., 2015. Paddy soil heavy metal contamination and uptake in rice plants from the adjacent area of Barapukuria coal mine, northwest Bangladesh. Arab J Geosci 8, 3391–3401. https://doi.org/10.1007/s12517-014-1480-1.
[42] Nagajyoti, P.C., Lee, K.D., Sreekanth, T.V.M., 2010. Heavy metals, occurrence and toxicity for plants: a review. Environ Chem Lett 8 (3), 199–216.
[43] Zhang, C., Nie, S., Liang, J., Zeng, G., Wu, H., Hua, S., et al., 2016. Effects of heavy metals and soil physicochemical properties on wetland soil microbial biomass and bacterial community structure. Sci Total Environ 557–558, 785–790. https://doi.org/10.1016/j.scitotenv.2016.01.170.
[44] Liang, J., Feng, C., Zeng, G., Gao, X., Zhong, M., Li, Xiaodong, et al., 2017. Spatial distribution and source identification of heavy metals in surface soils in a typical coal mine city, Lianyuan, China. Environ Pollut 225, 681–690. https://doi.org/10.1016/j.envpol.2017.03.057.
[45] Siddique, M.A.B., Alam, M.K., Islam, S., Diganta, M.T.M., Akbor, M.A., Bithi, U. H., et al., 2020. Apportionment of some chemical elements in soils around the coal mining area in northern Bangladesh and associated health risk assessment. Environ Nanotechnol, Monit Manag 14, 100366. https://doi.org/10.1016/j.enmm.2020.100366.
[46] Munoz-Olivas, R., Camara, C., 2001. Speciation related to human health. In: Ebdon, L., Pitts, L., Cornelis, R., Crews, H., Donard, O.F.X., Quevauviller, P. (Eds.), Trace Element Speciation for Environment. Food and Health. The Royal Society of Chemistry, pp. 331–353.
[47] Sun, Y., Zhou, Q., Xie, X., Liu, R., 2010. Spatial, sources and risk assessment of heavy metal contamination of urban soils in typical regions of Shenyang, China. J Hazard Mater 174, 455–462. https://doi.org/10.1016/j.jhazmat.2009.09.074.
[48] Oluyemi, E.A., Feuyit, G., Oyekunle, J.A.O., Ogunfowokan, A.O., 2008. Seasonal variations in heavy metal concentrations in soil and some selected crops at a landfill in Nigeria. Afr J Environ Sci Technol 2, 89–096.
[49] Fu, J., Zhao, C., Luo, Yupeng, Liu, C., Kyzas, G.Z., Luo, Yin, et al., 2014. Heavy metals in surface sediments of the Jialu River, China: their relations to environmental factors. J Hazard Mater 270, 102–109. https://doi.org/10.1016/j.jhazmat.2014.01.044.
[50] Siddiquee, N.A., Parween, S., Quddus, M.M.A., Barua, P., 2012. Heavy metal pollution in sediments at ship breaking area of Bangladesh. In: Subramanian, V. (Ed.), Coastal Environments: Focus on Asian Regions. Springer Netherlands, pp. 78–87.
[51] Rakib, M.R.J., Rahman, M.A., Onyena, A.P., Kumar, R., Sarker, A., Hossain, M.B., et al., 2022. A comprehensive review of heavy metal pollution in the coastal areas of Bangladesh: abundance, bioaccumulation, health implications, and challenges. Environ Sci Pollut Res 29, 67532–67558. https://doi.org/10.1007/s11356-022-22122-9.
[52] Baqui, M.A., 2012. Geological structure. In: Islam, Sirajul, Jamal, Ahmed A. (Eds.), Banglapedia: National Encyclopedia of Bangladesh, Second ed..,. Asiatic Society of Bangladesh.
[53] Islam, A.R.M.T., Hasanuzzaman, M., Islam, H.T., Mia, M.U., Khan, R., Habib, M. A., et al., 2020. Quantifying source apportionment, co-occurrence and ecotoxicological risk of metals from up-mid-downstream river segments, Bangladesh. Environ Toxicol Chem. https://doi.org/10.1002/etc.4814.
[54] Akbor, M.A., Rahman, M.M., Bodrud-Doza, M., Haque, M.M., Siddique, M.A.B., Ahsan, M.A., et al., 2020. Metal pollution in water and sediment of the Buriganga River, Bangladesh: an ecological risk perspective. Desalin Water Treat 193, 284–301.
[55] Ahsan, M.A., Satter, F., Siddique, M.A.B., Akbor, M.A., Ahmed, S., Shajahan, M., et al., 2019. Chemical and physicochemical characterization of effluents from the tanning and textile industries in Bangladesh with multivariate statistical approach. Environ Monit Assess 191, 1–24.
[56] Kumar, A., Ramanathan, A.L., Prabha, S., Ranjan, R.K., Ranjan, S., Singh, G., 2012. Metal speciation studies in the aquifer sediments of Semria Ojhapatti, Bhojpur District, Bihar. Environ Monit Assess 184, 3027–3042.
[57] Strbac, S., Grubin, M.K., Vasic, N., 2018. Importance of background values in assessing the impact of heavy metals in river ecosystems: case study of Tisza River, Serbia. Environ Geochem Health 40, 1247–1263. https://doi.org/10.1007/s10653-017-0053-0.

[58] Krauskopf, K.B., Bird, D.K., 1995. Introduction to Geo-Chemistry, third ed. McGraw-Hill, Inc, New York, p. 647.
[59] Kamau, J.N., 2002. Heavy metal distribution and enrichment at Port-Reitz Creek, Mombasa. West Indian Ocean J Mar Sci 1, 65–70.
[60] Schiff, K.C., Weisberg, S.B., 1999. Iron as a reference element for determining trace metal enrichment in Southern California coastal shelf sediments. Mar Environ Res 48, 161–176.
[61] Aprile, F.M., Bouvy, M., 2008. Distribution and enrichment of heavy metals at the Tapacurá River basin, northeastern Brazil. Braz J Aquat Sci Technol 12 (1), 8.
[62] Zhang, J., Liu, C.L., 2002. Riverine composition and estuarine geochemistry of particulate metals in China—weathering features, anthropogenic impact and chemical fluxes. Estuar Coast Shelf Sci 54, 1051–1070.
[63] Birch, G.F., Olmos, M.A., 2008. Sediment-bound heavy metals as indicators of human influence and biological risk in coastal water bodies. ICES J Mar Sci 65, 1407–1413.
[64] Muller, G., 1969. Index of geoaccumulation in sediments of the Rhine River. Geo J 2, 108–118.
[65] Loska, K., Wiechuła, D., Korus, I., 2004. Metal contamination of farming soils affected by industry. Environ Int 30, 159–165. https://doi.org/10.1016/S0160-4120(03)00157-0.
[66] Abrahim, G.M.S., Parker, R.J., 2008. Assessment of heavy metal enrichment factors and the degree of contamination in marine sediments from Tamaki Estuary, Auckland, New Zealand. Environ Monit Assess 136, 227–238.
[67] Ma, X., Zuo, H., Tian, M., Zhang, L., Meng, J., Zhou, X., et al., 2016. Assessment of heavy metals contamination in sediments from three adjacent regions of the Yellow River using metal chemical fractions and multivariate analysis techniques. Chemosphere 144, 264–272.
[68] Hakanson, L., 1980. An ecological risk index for aquatic pollution control.a sedimentological approach. Water Res 14, 975–1001. https://doi.org/10.1016/0043-1354(80)90143-8.
[69] Sadhu, K., Adhikari, K., Gangopadhyay, A., 2012. Assessment of heavy metal contamination of soils in and around open cast mines of Raniganj area, India. Int J Environ Eng Res 1, 77–85.
[70] Likuku, A.S., Mmolawa, K.B., Gaboutloeloe, G.K., 2013. Assessment of heavy metal enrichment and degree of contamination around the copper-nickel mine in the Selebi Phikwe Region, Eastern Botswana. Environ Ecol Res 1 (2), 32–40.
[71] Tomlinson, D.L., Wilson, J.G., Harris, C.R., Jeffrey, D.W., 1980. Problems in the assessment of heavy-metal levels in estuaries and the formation of a pollution index. Helgoländer Meeresunters 33, 566–575.
[72] Khan, R., Islam, M.S., Tareq, A.R.M., Naher, K., Islam, A.R.M.T., Habib, M.A., et al., 2020. Distribution, sources and ecological risk of trace elements and polycyclic aromatic hydrocarbons in sediments from a polluted urban river in central Bangladesh. Environ Nanotechnol, Monit Manag 14. https://doi.org/10.1016/j.enmm.2020.100318.
[73] Nemerow, N.L., 1985. Stream, Lake, Estuary, and Ocean Pollution. Van Nostrand Reinhold Publishing, New York, NY, USA.
[74] Benson, N.U., Enyong, P.A., Fred-Ahmadu, O.H., 2016. Trace metal contamination characteristics and health risks assessment of commelina africana L. and psammitic sandflats in the Niger Delta, Nigeria. Appl Environ Soil Sci 2016. https://doi.org/10.1155/2016/8178901.
[75] Yu, L., Zhang, B., Zhang, S.Q., 2004. Heavy metal elements pollution evaluation on the ecological environment of the Sanjiang Plain based on GIS. Chin. J Soil Sci 35 (5), 529–532.
[76] Yang, Z.P., Lu, W.X., Long, Y.O., Bao, X.H., Yang, Q.C., 2011. Assessment of heavy metals contamination in urban topsoil from Changchu n City, China. J Geochem Explor 108, 27–38. https://doi.org/10.1016/j.gexplo.2010.09.006.
[77] Jiang, X., Lu, W.X., Zhao, H.Q., Yang, Q.C., Yang, Z.P., 2014. Potential ecological risk assessment and prediction of soil heavy metal pollution around coal gangue dump. Nat Hazards Earth Syst Sci 14, 1599–1610.
[78] Al Anbari, R., Al Obaidy, A.H.M.J., Ali, F.H.A., 2015. Pollution loads and ecological risk assessment of heavy metals in the urban soil affected by various anthropogenic activities. Int J Adv Res 3 (2), 104–110.
[79] Cheng, H., Li, M., Zhao, C., Li, K., Peng, M., Qin, A., et al., 2014. Overview of trace metals in the urban soil of 31 metropolises in China. J Geochem Explor 139, 31–52. https://doi.org/10.1016/j.gexplo.2013.08.012.
[80] Zheng, N., et al., 2008. Characterization of heavy metal concentrations in the sediments of three freshwater rivers in Huludao City, Northeast China. Environ Pollut 154 (1), 135–142.
[81] Bai, J., et al., 2011. Assessment of heavy metal pollution in wetland soils from the young and old reclaimed regions in the Pearl River Estuary, South China. Environ Pollut 159 (3), 817–824.
[82] Proshad, R., Kormoker, T., Islam, S., 2018. Distribution, source identification, ecological and health risks of heavy metals in surface sediments of the Rupsa River, Bangladesh. Toxin Rev 40, 77–101. https://doi.org/10.1080/15569543.2018.1564143.
[83] MacDonald, D.D., Ingersoll, C.G., Berger, T.A., 2000. Development and evaluation of consensus-based sediment quality guidelines for freshwater ecosystems. Arch Environ Contam Toxicol 39, 20–31.
[84] Sahoo, P.K., Equeenuddin, S.M., Powell, M.A., 2016. Trace elements in soils around coal mines: current scenario, impact and available techniques for management. Curr Pollut Rep 2 (1), 1–14.
[85] Jiao, X., Teng, Y., Zhan, Y., Wu, J., Lin, X., 2015. Soil heavy metal pollution and risk assessment in Shenyang industrial district, Northeast China. PLoS One 10, e0127736.
[86] Adimalla, N., 2020. Heavy metals contamination in urban surface soils of Medak province, India, and its risk assessment and spatial distribution. Environ Geochem Health 42, 59–75. https://doi.org/10.1007/s10653-019-00270-1.
[87] Kamunda, C., Mathuthu, M., Madhuku, M., 2016. Health risk assessment of heavy metals in soils from witwatersrand gold mining basin, South Africa. Int J Environ Res Public Health 13. https://doi.org/10.3390/ijerph13070663.
[88] USEPA, 1989. Risk assessment guidance for superfund. In: Human health evaluation manual (Part A), Vol. 1. Office of Emergency and Remedial Response, Washington, DC.
[89] Chen, X., Liu, M., Ma, J., Liu, X., Liu, D., Chen, Y., et al., 2017. Health risk assessment of soil heavy metals in housing units built on brownfields in a city in China. J Soils Sediment 17, 1741–1750.
[90] Xu, Y., Dai, S., Meng, K., Wang, Y., Ren, W., Zhao, L., et al., 2018. Occurrence and risk assessment of potentially toxic elements and typical organic pollutants in contaminated rural soils. Sci Total Environ 630, 618–629.
[91] Deng, Y., Jiang, L., Xu, L., Hao, X., Zhang, S., Xu, M., et al., 2019. Spatial distribution and risk assessment of heavy metals in contaminated paddy fields–a case study in Xiangtan City, southern China. Ecotoxicol Environ Saf 171, 281–289.
[92] Adimalla, N., Wang, H., 2018. Distribution, contamination, and health risk assessment of heavy metals in surface soils from northern Telangana, India. Arab J Geosci 11, 1–15.
[93] USEPA (United States Environmental Protection Agency), 2002. Child Specific Exposure Factors Handbook; EPA-600-P-00–002B. National Center for Environmental Assessment, Washington, DC, USA.
[94] USEPA (United States Environmental Protection Agency), 2011. Exposure factors handbook 2011 Edition (Final), Office of emergency and remedial response, Washington, DC, USA.
[95] De Miguel, E., Iribarren, I., Chacón, E., Ordoñez, A., Charlesworth, S., 2007. Risk-based evaluation of the exposure of children to trace elements in playgrounds in Madrid (Spain). Chemosphere 66, 505–513. https://doi.org/10.1016/j.chemosphere.2006.05.065.
[96] Wang, J., Liu, G., Liu, H., Lam, P.K., 2017. Multivariate statistical evaluation of dissolved trace elements and a water quality assessment in the middle reaches of Huaihe River, Anhui, China. Sci Total Environ 583, 421–431.
[97] Bai, H., Hu, B., Wang, C., Bao, S., Sai, G., Xu, X., et al., 2017. Assessment of radioactive materials and heavy metals in the surface soil around the Bayanwula prospective uranium mining area in China. Int J Environ Res Public Health 14 (3), 300.
[98] USEPA, 2009. Risk-based Concentration Table. United States Environmental Protection Agency, Washington D.C., USA, Philadelphia PA.
[99] USEPA, 2010. Integrated risk information system (IRIS). United States Environmental Protection Agency, Washington D.C., USA.
[100] USEPA (United States Environmental Protection Agency), 2017. Integrated Risk Information System National Center for Environmental Assessment Office of Research and Development U.S.; Environmental Protection Agency: Washington, DC, USA.
[101] Ferreira-Baptista, L., De Miguel, E., 2005. Geochemistry and risk assessment of street dust in Luanda, Angola: A tropical urban environment. Atmos Environ 39, 4501–4512.
[102] USDOE (United States Department of Energy), 2011. The Risk Assessment Information System (RAIS); Department of Energy's Oak Ridge Operations Office (ORO): Oak Ridge, TN, USA.
[103] Neisi, A., Goudarzi, G., Akbar Babaei, A., Vosoughi, M., Hashemzadeh, H., Naimabadi, A., et al., 2016. Study of heavy metal levels in indoor dust and their health risk assessment in children of Ahvaz city, Iran. Toxin Rev 35, 16–23.
[104] Gad, A., Saleh, A., Farhat, H.I., Dawood, Y.H., Abd El Bakey, S.M., 2022. Spatial distribution, contamination levels, and health risk assessment of potentially toxic elements in household dust in Cairo City, Egypt. Toxics 10, 466. https://doi.org/10.3390/toxics10080466.
[105] Aendo, P., Netvichian, R., Thiendedsakul, P., Khaodhiar, S., Tulayakul, P., 2022. Carcinogenic risk of Pb, Cd, Ni, and Cr and critical ecological risk of Cd and Cu in soil and groundwater around the municipal solid waste open dump in central Thailand. J Environ Public Health 2022. https://doi.org/10.1155/2022/3062215.
[106] Zeng, F., Wei, W., Li, M., Huang, R., Yang, F., Duan, Y., 2015. Heavy metal contamination in rice-producing soils of Hunan province, China and potential health risks. Int J Environ Res Public Health 12, 15584–15593. https://doi.org/10.3390/ijerph121215005.
[107] Mugudamani, I., Oke, S.A., Gumede, T.P., 2022. Influence of urban informal settlements on trace element accumulation in road dust and their possible health implications in ekurhuleni metropolitan municipality, South Africa. Toxics 10, 253.
[108] Morgan, M.G., Henrion, M., Morris, S.C., Amaral, D.A., 1985. Uncertainty in risk assessment. Environ Sci Technol 19, 662–667.
[109] Carrington, C.D., Bolger, P.M., 1998. Uncertainty and risk assessment. Hum Ecol Risk Assess Int J 4, 253–257.
[110] Mesa-Frias, M., Chalabi, Z., Vanni, T., Foss, A.M., 2013. Uncertainty in environmental health impact assessment: quantitative methods and perspectives. Int J Environ Health Res 23, 16–30.
[111] Augustsson, A., Berger, T., 2014. Assessing the risk of an excess fluoride intake among Swedish children in households with private wells—expanding static single-source methods to a probabilistic multi- exposure, -pathway approach. Environ Int 68, 192–199. https://doi.org/10.1016/j.envint.2014.03.014.

[112] Karami, M.A., Fakhri, Y., Rezania, S., Alinejad, A.A., Mohammadi, A.A., Yousefi, M., et al., 2019. Non-Carcinogenic health risk assessment due to fluoride exposure from tea consumption in Iran using Monte Carlo simulation. Int J Environ Res Public Health 16, 4261. https://doi.org/10.3390/ijerph16214261.
[113] Shahrbabki, P.E., Hajimohammadi, B., Shoeibi, S., Elmi, M., Yousefzadeh, A., Conti, G.O., et al., 2018. Probabilistic non-carcinogenic and carcinogenic risk assessments (Monte Carlo simulation method) of the measured acrylamide content in Tah-dig using QuEChERS extraction and UHPLC-MS/MS. Food Chem Toxicol 118, 361–370. https://doi.org/10.1016/j.fct.2018.05.038.
[114] Harris, M.J., Stinson, J., Landis, W.G., 2017. A bayesian approach to integrated ecological and human health risk assessment for the South River, Virginia mercury-contaminated site. Risk Anal 37, 1341–1357. https://doi.org/10.1111/risa.12691.
[115] Habib, M.A., Islam, A.R.M.T., Bodrud-Doza, M., Mukta, F.A., Khan, R., Siddique, M.A.B., et al., 2020. Simultaneous appraisals of pathway and probable health risk associated with trace metals contamination in groundwater from Barapukuria coal basin, Bangladesh. Chemosphere 242, 125183.
[116] Islam, M.E., Reza, A.S., Sattar, G.S., Ahsan, M.A., Akbor, M.A., Siddique, M.A.B., 2019. Distribution of arsenic in core sediments and groundwater in the Chapai Nawabganj district, Bangladesh. Arab J Geosci 12 (3), 99. https://doi.org/10.1007/s12517-019-4272-9.
[117] Reddy, M.S., Basha, S., Sravan Kumar, V.G., Joshi, H.V., Ramachandraiah, G., 2004. Distribution, enrichment and accumulation of heavy metals in coastal sediments of Alang–Sosiya ship scrapping yard, India. Mar Pollut Bull 48, 1055–1059.
[118] Yilmaz, A., Karacik, B., Yakan, S.D., Henkelmann, B., Schramm, K.W., Okay, O.S., 2016. Organic and heavy metal pollution in shipbreaking yards. Ocean Eng 123, 452–457. https://doi.org/10.1016/j.oceaneng.2016.06.036.
[119] Neser, G., Kontas, A., Ünsalan, D., Uluturhan, E., Altay, O., Darilmaz, E., et al., 2012. Heavy metals contamination levels at the Coast of Aliaĝa (Turkey) ship recycling zone. Mar Pollut Bull 64, 882–887. https://doi.org/10.1016/j.marpolbul.2012.02.006.
[120] Kara, M., Dumanoğlu, Y., Altıok, H., Elbir, T., Odabası, M., Bayram, A., 2014. Spatial distribution and source identification of trace elements in topsoil from heavily industrialized region, Aliaga, Turkey. Environ Monit Assess 186, 6017–6038. https://doi.org/10.1007/s10661-014-3837-z.
[121] Saher, N.U., Siddiqui, A.S., 2019. Occurrence of heavy metals in sediment and their bioaccumulation in sentinel crab (Macrophthalmus depressus) from highly impacted coastal zone. Chemosphere 221, 89–98. https://doi.org/10.1016/j.chemosphere.2019.01.008.
[122] Ganugapenta, S., Nadimikeri, J., Chinnapolla, S.R.R.B., Ballari, L., Madiga, R., Nirmala, K., et al., 2018. Assessment of heavy metal pollution from the sediment of Tupilipalem Coast, southeast coast of India. Int J Sediment Res 33 (3), 294–302.
[123] Antizar-Ladislao, B., Mondal, P., Mitra, S., Sarkar, S.K., 2015. Assessment of trace metal contamination level and toxicity in sediments from coastal regions of West Bengal, eastern part of India. Mar Pollut Bull 101 (2), 886–894.
[124] Tunca, E., Aydin, M., Sahin, U.A., 2018. An ecological risk investigation of marine sediment from the northern Mediterranean coasts (Aegean Sea) using multiple methods of pollution determination. Environ Sci Pollut Res 25, 7487–7503. https://doi.org/10.1007/s11356-017-0984-0.
[125] Ungureanu, T., Iancu, G.O., Pintilei, M., Chicoş, M.M., 2017. Spatial distribution and geochemistry of heavy metals in soils: a case study from the NE area of Vaslui county, Romania. J Geochem Explor 176, 20–32.
[126] Fan, S., Wang, X., Lei, J., Ran, Q., Ren, Y., Zhou, J., 2019. Spatial distribution and source identification of heavy metals in a typical Pb/Zn smelter in an arid area of northwest China. Hum Ecol Risk Assess. https://doi.org/10.1080/10807039.2018.1539640.
[127] Luo, X.S., Yu, S., Zhu, Y.G., Li, X.D., 2012. Trace metal contamination in urban soils of China. Sci Total Environ 421–422, 17–30. https://doi.org/10.1016/j.scitotenv.2011.04.020.
[128] Qing, X., Yutong, Z., Shenggao, L., 2015. Assessment of heavy metal pollution and human health risk in urban soils of steel industrial city (Anshan), Liaoning, Northeast China. Ecotoxicol Environ Saf 120, 377–385. https://doi.org/10.1016/j.ecoenv.2015.06.019.
[129] Plum, L.M., Rink, L., Haase, H., 2010. The essential toxin: impact of zinc on human health. Int J Environ Res Public Health 7 (4), 1342–1365.
[130] Li, Z., Ma, Z., van der Kuijp, T.J., Yuan, Z., Huang, L., 2014. A review of soil heavy metal pollution from mines in China: pollution and health risk assessment. Sci Total Environ 468, 843–853.
[131] IAEA, 1990. Guidebook on applications of radiotracers in industry. Technical Report Series No. 316.
[132] GESAMP (Joint Group of Experts on the Scientific Aspects of Marine Environmental Protection), IMO/FAO/IJNESCO/WMO/IAEA/UN/IJNEP, 1982. The health of the oceans. Rep Stad GESAMP 15, 108.
[133] Cox, P.A., 1989. The elements: their origin, abundance and distribution. Oxford University Press, London.
[134] Iwegbue, C.M.A., Lari, B., Osakwe, S.A., Tesi, G.O., Nwajei, G.E., Martincigh, B.S., 2018. Distribution, sources and ecological risks of metals in surficial sediments of the Forcados River and its Estuary, Niger Delta, Nigeria. Environ Earth Sci 77, 227. https://doi.org/10.1007/s12665-018-7344-3.
[135] USEPA, 1999. A Risk Assessment–Multiway Exposure Spreadsheet Calculation Tool. United States Environmental Protection Agency, Washington, DC, USA.
[136] Mashiatullah, A., Chaudhary, M.Z., Ahmad, N., Javed, T., Ghaffar, A., 2013. Metal pollution and ecological risk assessment in marine sediments of Karachi Coast, Pakistan. Environ Monit Assess 185, 1555–1565. DOI 10.1007/s10661-012-2650-9.
[137] Karimi, A., Naghizadeh, A., Biglari, H., Peirovi, R., Ghasemi, A., Zare, A., 2020. Assessment of human health risks and pollution index for heavy metals in farmlands irrigated by effluents of stabilization ponds. Environ Sci Pollut Res 27, 10317–10327.
[138] Lin, Y., Fang, F., Wang, F., Xu, M., 2015. Pollution distribution and health risk assessment of heavy metals in indoor dust in Anhui rural, China. Environ Monit Assess 187, 565.
[139] USEPA (United States Environmental Protection Agency), 1996. Soil Screening Guidance: Technical Background Document; Office of Soild Waste and Emergency Response: Washington, DC, USA.